12

Final Report

on the

REGIONALIZATION OF THE ARCTIC REGION, SIBERIA AND EURASIAN CONTINENTAL AREA

Sponsored by

Advanced Research Projects Agency

ARPA Order No. 1827

Principal Investigator: Professor Leon Knopoff
(Telephone No: 213-825-1885)

Program Manager: Mr. William J. Best
(Telephone No: 202-694-5456)

Contract Number: Air Force Contract F44620-73-C-0048

Amount of Contract: $164,986

Effective Dates of Contract: March 1, 1973 to May 31, 1976

Program Code: 4F10

Institute of Geophysics and Planetary Physics
University of California, Los Angeles

May 31, 1976

TABLE OF CONTENTS

DISCLAIMER NOTICE

THIS DOCUMENT IS THE BEST QUALITY AVAILABLE.

COPY FURNISHED CONTAINED A SIGNIFICANT NUMBER OF PAGES WHICH DO NOT REPRODUCE LEGIBLY.

TECHNICAL REPORT SUMMARY

In this investigation, our first purpose is the regionalization of the Arctic region, Siberia and the Eurasian continental area using seismic surface waves. This regionalization will determine the structural properties of the upper few hundred kilometers of the earth, and the variation of these properties from one subregion to another in the area under investigation. Once the structural properties in the various regions have been obtained, our second purpose is to apply optimized computer techniques to the computation of accurate theoretical seismograms for any hypothetical type of source located anywhere within this continental area. These theoretical seismograms can be applied directly to the discrimination problem by comparing seismograms, computed for both earthquakes and underground explosions, with the actual recorded seismogram.

Regionalization. The first technical problem to be dealt with, which is complete, is the computation of experimental phase velocity curves for surface waves traversing all of the regions under investigation.

The phase velocity curves were obtained with the single-station phase velocity method, which is described in the main text of this report. Briefly, the method involves scanning our microfilm library of World Wide Standardized Seismographic Network (WWSSN) records for earthquakes which: (1) occurred within, or on the perimeter of, the area of interest, (2) produced good long-period surface wave records at WWSSN stations for which the epicenter-to-station lines lie within the regions being investigated, and (3) generated good, large recordings at a sufficient

number of stations to ensure an accurate fault plane solution. When a suitable earthquake has been found, an extensive data processing and data reduction system is applied to transform the data into phase velocity curves for each of the selected epicenter-to-station lines through the area of interest.

The complete set of phase velocity curves (for fundamental-mode Rayleigh waves recorded by the WWSSN instruments), which will be required for the regionalization of the Arctic region, Siberia, and the Eurasian continental area, consists of about 50 dispersion curves. Based on this data set, we have just obtained our first really successful regionalization of the structures in the area under investigation. The computer programs, upon which the inversion of the data for structural information is based, were first used successfully in the regionalization of the Pacific Ocean area (Kausel, 1972; Leeds, 1973; Kausel, Leeds and Knopoff, 1974; Leeds, Knopoff and Kausel, 1974).

Our attack on the inversion problem has been a three-part effort: (1) the regionalization of Siberia and the Eurasian continental area, using only the data for paths limited to these regions; (2) the regionalization of the Arctic area, again, using only the data for paths limited to this region; and (3) the final regionalization of Siberia, the Eurasian continental area, and also the Arctic region, using the entire set of data we have available, including many profiles having both continental and oceanic segments between epicenter and station. We have completed the first successful inversion process relative to part (1), and reduced the data from part (2) to obtain the phase velocity for the subregion of major interest in this area; the execution of part (3) is planned

for our next contract year.

From our preliminary regionalization work on the continental areas, we can draw a few conclusions already. First, we note that the properties of much of the Asiatic upper mantle, averaged over long trans-Eurasian distances, are highly consistent with those of young stable regions observed elsewhere (Knopoff, 1972; Fouda, 1973; Knopoff and Fouda, 1974). Second, the Tibetan plateau has an extremely thick crust, perh s as great as 80 km from surface to Moho. Third, the A.pide folded belt of Iran and Turkey has an extraordinarily well-developed low-velocity channel in the mantle, of remarkable contrast to the lid above. The principal problem in the inversion has been the construction of the boundaries to the geological provinces, for which only incomplete information is found in the literature. This difficulty is what has led us to the idea of repeating parts (1) and (2) of our scheme of regionalization. The detailed (preliminary) results of our inversion are given on pages 21-38.

Theoretical Seismograms. The second phase of our contract work -- computing realistic theoretical seismograms at the WWSSN stations, and especially at the new high-gain, wideband installations (Pomeroy et al., 1969; Molnar et al., 1969; Savino, McCarry and Hade.1972) at Kongserg, Norway (KON), Toledo, Spain (TOL), Eilat, Israel (EIL), Chiengmai, Thailand (CHG), and Matsushiro, Japan (MAT), for arbitrary seismic and explosive sources within the area under investiagation -- is, of course, dependent upon the availability of the final regionalization

from the first section of our investigation. To prepare for this work, we have concentrated upon improving our existing algorithms and computer programs for generating theoretical seismograms for highly realistic models of the earth. In this, we have succeeded to the extent that only the problem of the lateral heterogeneity, over the area of investigation, remains as an important consideration in the further development of our system for computing these theoretical time series. These statements apply to the Love, or torsional waves excited by earthquakes and explosions; the parallel development of our algorithms and computer programs for Rayleigh, or spheroidal waves on a spherical, gravitating earth is currently one of the main efforts under this contract.

The work published out of our section has become quite voluminous (see following Technical Report) in the subjects -- dispersion computations, attenuation computations, structural transformations, eigenfunction characteristics, effects of sphericity, point-source response computations --upon which efficient construction of accurate, multimode theoretical seismograms for realistic models of the earth's structure are based.

Our original work with theoretical seismograms concerned the multimode surface wave phases Lg (Knopoff, Schwab and Kausel, 1973; Knopoff et al., 1974) and Sa (Schwab et al., 1974). Relative to discrimination studies, however, it is desirable to have body wave phases also available on the theoretical seismograms; this is one direction of our current work; the other is improvement in efficiency, control of accuracy, and increased

power and flexibility of the computational algoritms and computer programs. Our first successes in generating complete seismograms, i.e., body and surface waves on the same record, were reported by Nakanishi et al., (1975), Nakanishi, Schwab and Kausel (1976), and Nakanishi, Schwab and Knopoff (1976). This work includes the summation of eight modes, and the computations are applied to a continental structure; our first multimode time series for an oceanic structure (Kausel, Schwab and Mantovani, 1976) also forms part of this research. Multimode theoretical seismograms containing body wave phases have been generated in the past (Satô, Usami and Landisman, 1968); however, these time series were limited to ultralong periods. The important point of our present results is that, owing to the new high efficiency of our algorithms, we have been successful in extending the period content of the theoretical seismograms down through the range covered by the long-period instruments of the WWSSN. Thus, we can generate the theoretical time series which, for the first time we believe, permits us to begin thinking about the comparison of theoretical seismograms with the entire records obtained at the WWSSN and the new high-gain, wideband installations. Our current level with these theoretical-numerical techniques permits the generation of time series with a combination of eleven modes, and for the arbitrary specification of source depth as well as the other focal parameters. The results of this level of our system are given by Mantovani et al. (1976a, 1976b). Our immediate goal in this work is the extension to the combination of fifteen, and finally twenty, modes to form these theoretical time series.

TECHNICAL REPORT

I. Purposes of this project

The first purpose of our project is to determine the structural properties, and the variation of these properties, throughout the regions under investigation. The technique used for this purpose is the study of the localized properties of surface wave propagation in the Arctic region, Siberia and the Eurasian continental area. Regionalization techniques, which have recently been developed at UCLA, are then applied to the long-period surface-wave dispersion data obtained from the single-station method, and localized structural information results from this application. The regions of high seismicity within and around the region to be investigated are quite favorably located for the application of the single-station technique. The dense set of WWSSN stations located around the perimeter of the region ensures that we can acquire sufficient data for the application of our regionalization methods.

The second purpose of our project is then to apply optimized computational techniques to the problem of computing complete, accurate theoretical seismograms of events excited by both earthquakes and explosive sources, within the area under investigation, and recorded at the WWSSN and high-gain, wide-band stations surrounding these regions. The accuracy of the computed theoretical seismograms, and hence their value (relative to the discrimination problem) for comparison with experimentally recorded events, is dependent upon the results of the first part of our study, i.e., an accurate knowledge of the regional

structural properties of Siberia, the Eurasian continental area, and the Arctic region.

II. Review of scientific background

Regionalization. Since the single-station surface wave method allows all stations to be located at the edge of the region under investigation, this technique is ideal for the proposed study. Brune et al. (1960) were the first to describe the single-station method. Knopoff and Schwab (1968) corrected and extended this description to take into account the frequency dependence of the apparent initial phase of the source. Based on the Thomson (1950)-Haskell (1953) matrix formulation for surface wave propagation, Harkrider (1964) developed the theory for treating the surface wave response to buried point-source singlets. Ben-Menahem and Toksöz (1963) then developed the formalism, in terms of the singlet response, for representing the displacement field of an arbitrary force system in a multilayered medium; and Ben-Menahem and Harkrider (1964) applied this formalism to obtain the surface wave response to point-source couples and double couples. Harkrider (1970) later made certain corrections and improvements in these last results. The far-field response to realistic, displacement-dislocation faulting was shown to be equivalent to the point-source, double-couple force replacement in an unfaulted medium (Maruyama, 1963; Burridge and Knopoff, 1964), and the single-station method was on firm theoretical ground for flat, multilayered media. By means of transformation techniques (Biswas and Knopoff, 1970; Schwab and Knopoff, 1972), it is possible to convert point-source programs for a flat structure into those

useful for treating sources in a spherical structure (Kausel and Schwab, 1973). These programs for the surface wave response to displacement dislocations in a radially heterogeneous sphere are now a part of our program library. We are using, improving, and optimizing these programs as part of the present project.

Techniques for obtaining structural information from dispersion data were discussed by Knopoff (1961,1962), and the first programming of the inversion procedure appears to have been carried out by Dorman and Ewing (1962). These papers described attempts to obtain the single best structure for fitting the experimental data. Subsequent efforts were mainly concerned with finding the set of structural models which fit the data to within the experimental accuracy (Keilis-Borok and Yanovskaya, 1967; Press, 1968,1969). This work led to the programming, under the direction of Knopoff and Keilis-Borok, of the Hedgehog inversion package (Biswas and Knopoff, 1974; Knopoff and Schlue, 1972). This technique involves seeking structures, which satisfy the data to within the experimental accuracy, by means of a pointwise search throughout a multidimensional parameter space. This package is efficient enough for routine application to surface wave dispersion data. We have now introduced variational parameters into the procedure, which has resulted in a significant increase in computational efficiency. A description of the ideas involved in this improvement is given by Wiggins (1972) and Jackson (1972); the technique takes into account the redundancy in the data as well as numerical instabilities in the solution.

The single-station, surface wave regionalization of an area is based on the assumption of great-circle propagation paths, and the assumption that the phase travel time from epicenter to station is just the sum of the travel times through the subdivisions of the laterally heterogeneous region (Knopoff, 1969). This permits the regionalization to be expressed at each frequency as a system of inhomogeneous equations; for each path, the total travel time is the inhomogeneous term, the distances through the subdivisions are the coefficients, and the slownesses in the subdivisions are the unknowns. Santô [equation (1), 1961b] applied this technique to the Pacific, using group travel times and group slownesses but, due to considerations involving uniqueness of inversion (Pilant and Knopoff, 1970), we prefer phase travel time and phase slownesses. The solution of this system of equations yields the experimental phase slownesses associated with each of the subdivisions, in principle; however, the above procedure represents a version of the computer program which is not pedagogically acceptable. Instead, we prefer to consider the model parameters as the primary unknowns in the inversion and to use the phase velocities therefrom.

The initial, large scale, lateral regionalization of a portion of the earth by means of single-station surface wave studies was performed by Santô (1960a; 1960b; 1961a; 1961b) in an investigation of the Pacific Ocean basin. The bandwidth of his recordings and his data processing techniques limited almost all of his dispersion results to periods less than about 40 seconds; Santô's regionalization did not yield structural

information below the crust and lid of the mantle. Our current data processing techniques (Biswas, 1971), and the availability of a nearly complete library of long-period seismograms from the WWSSN stations, have made it possible to extend the lateral regionalization to a depth of about 250 km. The first application of our single-station regionalization techniques was an investigation of the upper mantle structure in the Pacific Ocean Basin (Leeds, 1973).

To exhibit the potential power of this technique, a brief summary of our work with the structure in the Pacific Ocean Basin will be useful: The results of the work of Kausel (1972) showed an apparently continuous gradation of Rayleigh-wave phase velocities from low values observed on paths close to the East Pacific Rise to relatively high values on paths in the oldest parts of the lithosphere. Leeds (1973) increased the body of data and performed the first successful inversion of the data, assuming that regional variations in structure were correlated with lithospheric age; that study took into account bathymetry and available crustal information. The number of degrees of freedom in the data was found to be remarkably small, despite the large number of phase-velocity determinations. The inversion led to the conclusion that the data set did not permit one to obtain detailed information concerning the bottom of the low-velocity channel. Furthermore, the lithosphere increased in thickness monotonically with age: at the ridge crest, the lithosphere has almost zero thickness. This is thus the explanation for the observation

that the phase velocities change systematically with distance from the ridge crest. The model of lithospheric thickness as a function of spreading age is consistent with the model wherein the lithosphere-asthenosphere interface is at the solidus for wet peridotite. The results of the Kausel and the Leeds Ph.D. theses, as well as some later conclusions, now appear in the literature: Kausel, Leeds and Knopoff (1974), Leeds, Knopoff and Kausel (1974), and Leeds (1975). These single-station regionalization techniques are being refined for use in the present project.

Upper mantle studies in Eurasia appear to have suffered due to the Soviet seismologists' lack of efficient long-period instruments. Also, their extensive program in deep seismic sounding has undoubtedly served to focus interest upon crustal studies, to the detriment of sub-Moho investigations. The review by Arkhangel'skaya (1960) discusses the foreign and domestic surface wave studies performed in Eurasia prior to 1960. The early Soviet studies discussed in this review, as in the later studies to be mentioned here, were limited to short-period investigations -- usually less than 40 seconds -- and were concerned mainly with determining crustal properties. Of the early Soviet studies, which more or less paralleled the work in the west, the investigations of Savarensky and Ragimov (1958; 1959),

Savarensky, Solov'eva and Shechkov (1959), and Savarensky and Sikharulidze (1959) clearly demonstrate this predominant interest in crustal features. The subsequent work by Popov (1960), Shechkov (1961), Savarensky and Shechkov (1961), Shechkov and Solov'eva (1961), and Shechkov (1964) indicated that the Soviet surface wave investigations would remain focused on crustal studies, and ideed, this has proven to be the case up through the most recent Soviet surface wave literature available to us (Savarensky and Peshkov, 1968; Sikharulidze and Makharadze, 1968; Savarensky et al., 1969, Shechov, 1970).

All of these crustal studies, as well as Santô's (1962, 1965a; 1965b) short-period regionalization efforts should be valuable in assisting the determination of which shallow structures to combine with our trial parameterizations for the deep structures in the inversion portion of the present investigation.

Theoretical seismograms. Relative to the discrimination problem, probably the most important feature in the calculation of theoretical seismograms which requires improvement over previously existing systems for such computations is the capability of including short-period information while retaining both body- and surface-wave arrivals on the computed seismograms. In this context, by "short-period" we refer to the period range covered by the long-period instruments of the WWSSN installations. In practical terms, the successful accomplishment of this required improvement is dependent upon highly-optimized techniques for obtaining multimode dispersion-attenuation information for realistic models of the earth, i.e., spherical, radially heterogene-

ous, anelastic models.

Such optimization work has been one of the main interests in our laboratory for several years. The results of our early work, based on the Thomson (1950)-Haskell (1953) technique and on Knopoff's (1964) method for treating flat-layered structures, are reported by Schwab (1970) and Schwab and Knopoff (1970;1971; 1972;1973). The complete results of our work on spherical-to-flat-structure transformation techniques, which permit the use of the optimized flat-structure programs in dispersion-attenuation computations for spherical models of the earth, are given by Biswas and Knopoff (1970), Schwab and Knopoff (1971;1972;1973), and Kausel and Schwab (1973). In this last reference, we have also given our initial outline of the approach we have adopted to handle the synthesis of multimode seismograms once the dispersion, attenuation, source, and excitation functions have been specified. This approach has been derived from the basic theory, which shows that the entire theoretical seismogram for a dislocation source in a spherical earth can be expressed as a simple sum of normal mode contributions, as given by Saito (1967) and Takeuchi and Saito (1972). Our first successes with the system we developed for generating theoretical seismograms were applied to the interpretation of the seismic phase Lg (Knopoff, Schwab and Kausel, 1973; Knopoff et al., 1974). This phase is, as we demonstrated in these publications, a multimode interference phenomenon which belongs to the surface wave portion of the seismogram. It is only under the present contract (see following section) that we have developed the system, which is the

first we are aware of for synthesizing entire seismograms for realistic models of the earth, where both body waves and surface waves appear on the same record, and where the period content of the record extends down through the range covered by the long-period instruments of the WWSSN. Earlier work of this type, which was performed with simplified models of the earth, is summarized by Alterman and Loewenthal (1972). Satô, Usami and Landisman (1968) describe the computation of complete theoretical seismograms for realistic models of the earth. However, their results are limited to ultralong periods.

III. Objectives, methods and results.

Data collection. To perform the regionalization of the area under investigation with the single-station method, we must know the orientation of the fault plane, depth of focus, and the direction of displacement dislocation at the focus. These provide calculable corrections due to apparent initial phase of the Rayleigh wave signal. Our current interpretation procedures, for obtaining structural parameters as a function of depth, are based solely on the phase velocity dispersion of the isolated fundamental mode; hence, this correction can be quite important in our regionalization studies. One problem which is associated with accurate determination of the apparent initial phase is the dependence of this value on a precise knowledge of the structural parameters beneath the epicenter, which are used to calculate this correction. To determine the importance of this dependence, we have performed a detailed analysis, the results of which are reported by Frez and Schwab (1976, copy of page proofs appended).

Our recent large-scale regionalization work (Biswas, 1971; Kausel,1972; Leeds,1973; Fouda,1973; Kausel et al.,1974; Leeds et al.,1974; Knopoff and Fouda,1974) has shown the value and ease of handling of seismic records of fundamental mode Rayleigh waves. Our efforts in the present study have therefore been focused on this well-tested approach.

The long-period records from the 47 WWSSN stations which border the region of interest have been used in the study. The locations of these stations are shown in Figure 1. We have also obtained several seismograms (through World Data Center B) of Soviet records made in Central Asia on experimental long-period instruments. However, the precision of these recording plus an uncertain

impulse response has not permitted us to make use of these recordings.

In order to obtain the desired long-period information from WWSSN records, it is necessary to use shocks of relatively large magnitude, yet small enough to be on-scale at the stations of the network. An example of the intermediate-magnitude seismicity of the area is given in Figure 2. The epicenters are plotted for earthquakes having magnitudes between 5.9 and 6.6, which occurred during the interval from February, 1963 to February, 1967. The choice of this range of magnitudes is governed by two considerations. First, experience has shown that good long-period surface wave information requires events with magnitudes above a certain value and, of course, a shock which is so large as to send the instrument off scale is useless for our purposes. Second, the application of the single-station method requires knowledge of the focal mechanism. We must therefore use events large enough to allow us to obtain an accurate fault plane solution for each event we select for processing. In addition to the epicenters shown in Figure 2, there are regions of high seismicity along the eastern border of the Kamchatka peninsula and along the Aleutian arc, which may provide useful events for this study.

With such a dense set of stations around the area to be studied, and with the regions of high, intermediate -magnitude seismicity located within and around the area, there has been no problem in obtaining sufficient data for the project. It is interesting to note that the area is almost completely encircled: There is only one significant gap -- between Japan and Alaska -- where stations do not exist. However, this gap is a region of high seismicity which, in the single-station

sense, is equivalent to having a high station density in the region.

There are far too many epicenter-to-station paths to show individually, but the limits of the area, which we have covered with a sufficiently dense set of paths, are shown in Figure 3 by the solid lines. The solid regions are those of high, large-magnitude seismicity.

The first event processed has the following USCGS specification:

March 7, 1966 -- 21:29:17.4 GMT, 37.3°N, 114.9°E,

$h = 33$ km, $M = 6.0$.

Our fault plane solution for this event is given in Figure 4. This first-motion information restricts the fault plane solution sufficiently well so that only this information is needed to determine the required focal specification. The location of the epicenter and epicenter-to-station paths which were selected for processing are given in Figure 5.

The computation of the correction for the apparent initial phase requires the specification of the strike of the fault plane ϕ , its dip δ and the direction of slip λ , and the depth to the focus h. These parameters are shown in the fault-plane geometry given in Figure 6. For the above event, our fault-plane solution yields

$\phi = 122°$ east of north

$\delta = 82°$

$\lambda = 90°$

and inspection of the Rayleigh-wave amplitude spectra indicates

a focal depth of

$h = 14.5$ km .

The second event selected for processing has the following USCGS specification:

August 25, 1964 -- 13:47:20.6 GMT, 78.2°N, 126.6°E ,

$h = 50$ km, $M = 6.1$.

The location of the epicenter, and the epicenter-to-station paths which were selected for processing are given in Figure 7. The fault-plane solution for this event was given by Sykes (1967) as

$\phi = 4°$ east of north

$\delta = 58°$ west

for one possible fault plane, and

$\phi = 22°$ west of north

$\delta = 54°$ east

for the other.

Our result for this event is

$\phi = 15°$ west of north

$\delta = 58°$ west

$\lambda = 260°$

$h = 11.5$ km .

The angles ϕ and δ are well-constrained by the first-break fault-plane solution given in Figure 8; the additional information contained in the Rayleigh-wave amplitude radiation patterns, which are shown in Figure 9, is required to fix λ and h .

The epicenter and propagation paths of the third event selected:

December 26, 1964 -- 14:30:29.1 GMT, 51.8°N, 156.8°E,

h = 136 km, M = 5.7 (USCGS)

are shown in Figure 10, and the results of our first-motion fault plane analysis for this event are given in Figure 11.

The epicenter and propagation paths for the fourth event selected:

March 31, 1969 -- 07:15:54.4 GMT, 27.7°N, 34.0°E,

h = 33 km, M = 6.0 - 6.8

are given in Figure 12.

The epicenter and propagation paths for the fifth event selected:

April 25, 1966 -- 23:22:49.3 GMT, 49.3°N, 69.2°E,

h = 8 km, M = 5.3

are given in Figure 20. The results of the first-motion fault plane analysis for this event are obtained from Zakharova et. al. (1971):

ϕ = 55° west of north

δ = 70°

λ = 90°

The sixth event we have used is a Chinese nuclear explosion which has the following USCGS specification :

October 14, 1970 -- 07:29:58.6 GMT, 40.9°N, 89.4°E

The source and propagation paths for this event are shown in Figure 20. We assume the focal mechanism of the source is that of a simple explosion source at the surface of the earth.

The combined Rayleigh wave propagation paths are shown in Figure 17, where the continental areas are emphasized, and in Figure 18, where the Arctic region is emphasized

Two events with approximately the same epicenter were also processed. These are

February 6, 1965 -- 01:40:33.2 GMT, 53.2°N, 161.9°W, h = 33 km, M = 6.4 - 6.7

and

February 6, 1965 -- 16:50:29 GMT, 53.3°N, 161.8°W, h = 33 km, M = 6.1 - 6.6 .

The paths are shown in Figure 13; the fault plane solutions are given in Figure 14.

Two events with approximately the same epicenter were the final ones processed. The USCGS specifications are:

February 5, 1965 -- 09:32:09.3 GMT, 52.3°N, 174.3°E, h = 41 km, M = 5.9 - 6.5

and

February 6, 1965 -- 04:02:53 GMT, 52.1°N, 175.7°E, h = 35 km, M = 5.9 - 6.0 .

These paths are shown in Figure 15; the fault plane solutions are given in Figure 16.

The complete list of events used in our studies is as follows:

Hsingtai	Mar. 7, 1966	21:29:17.4	37.3°N	114.9°E
Lena River	Aug.25, 1964	13:47:20.6	78.2°N	126.6°E
Kamchatka	Dec.26, 1964	14:30:29.1	51.8°N	156.8°E
Red Sea	Mar.31, 1969	07:15:54.4	27.7°N	34.0°E
Tashkent	Apr.25, 1966	23:22:49.3	41.3°N	69.2°E
Lop Nor	Oct.14, 1970	07:29:58.6	40.9°N	89.4°E
East.Aleut.	Feb. 6, 1965	01:40:33.2	53.2°N	161.9°W
East.Aleut.	Feb. 6, 1965	16:50:23.6	53.3°N	161.8°W
West.Aleut.	Feb. 5, 1965	09:32:09.3	52.3°N	174.3°E
West.Aleut.	Feb. 6, 1965	04:02:53	52.1°N	175.7°E

Two interesting points concerning the data-processing techniques have come to light during the present study. Both involve the accuracy of the digitizations of the recorded events. First, most of the event records we have used are about as large as they could be without going off scale. This has necessitated a change in our data processing techniques which should be noted for the information of others involved in this type of work.

In the past, our standard procedure, when working with smaller-amplitude recordings, has been to make copies of events from 35 mm microfilm records of the WWSSN seismograms. These copies are made with a standard microfilm reader-printer (Itek 18.24 Reader-Printer), and the events are then digitized from these copies. We followed this procedure during the initial phase of the present investigation, but later became concerned about the possibility of distortion in the copying process. Our tests comparing the phase velocity results obtained from full-size record copies provided by NOAA with the results obtained from our microfilm copies shows this concern to be valid. Our conclusion is that, when working with large-amplitude recordings sich as those employed in the present study, one must use full-size record copies; one must not use a microfilm copier which forces the analysis to use several prints, spliced together, to form the record copy from which the digitization is obtained.

The second point which arose, involving accuracy of digitization, concerns the fact that the direction of swing of the galvanometer may not be parallel to the axis of the recordiing drum (James and Linde,1971). Although James and Linde (1971) term this phenomenon "a source of major error in digital analysis of WWSSN seismograms", our tests show the effect to be negligible on the phase velocities computed using the single-station method for epicenter-station separations of a few thousand kilometers. In the case of the poorest galvanometer alignment we encountered -- about triple the normal ramp slope of 0.3° -- we found only negligible differences between the phase velocity curve obtained with the correct digitization base line, and the curve obtained with the normal ramp as a base line (Leeds, unpublished).

Regionalization. Our preliminary efforts at the regionalization of the area under investigation were focused on the continental regions. Sample phase velocity results are given in Figure 19, which illustrates the variation in dispersion for different propagation paths.

We have obtained phase velocity data for most paths over a period range extending from about 30 or 38 sec, in most cases, to as long as 357 sec in a few rare cases. The instrumental response at 357 sec is sufficiently unreliable that we have used phase velocity information from observations of the free oscillation spectrum of the earth to determine if the phase velocity values and their first derivatives were approximately correct. Measured values that were in significant disagreement with values from the free mode spectrum were rejected. For our present level of inversion, we have used periods only up to 250 sec.

The specific period ranges, which were used in the present inversion, are shown in Table 1.

The phase velocities from the five earthquakes and one nuclear explosion for the 32 paths in question (Figure 20) appear to assort themselves into two groups (Figures 21 and 22). The paths with higher phase velocities are generally those that cross the stable platforms and shields (such as paths from the Hsingtai earthquake to Scandinavian (KEV) and German (STU) stations; typical of the lower-velocity group is the phase velocity on the paths from the Red Sea earthquake to the southern Asiatic stations (SHL, MAN, etc.) . Phase velocities for typical shield regions and young stable continental regions (Biswas and Knopoff,1974) are shown for comparison. The incompatibility of most of the phase velocity observations for Eurasian paths with the "standard" curves for homogeneous regions testify to the inhomogeneous nature of the Eurasian continent.

The first step in the structural analysis required the division of the area into subregions, in each of which the structural parameters are assumed to be laterally homogeneous. Our first subdivision is shown in Figure 23, and was based on the use of the worldwide tectonic map (Khain and Muratov,1969). Parts of this map are too detailed for our purposes; however, they provide the basis for our regionalization. We have subdivided the Eurasian area into six regions which represent structural averages of a broad nature. In the subdivision, we have been guided by the development of continental regionalization based on inversion of surface wave phase velocity data (Knopoff,1972). We have used the tectonic and heat-flow maps to indicate where certain typical

TABLE 1

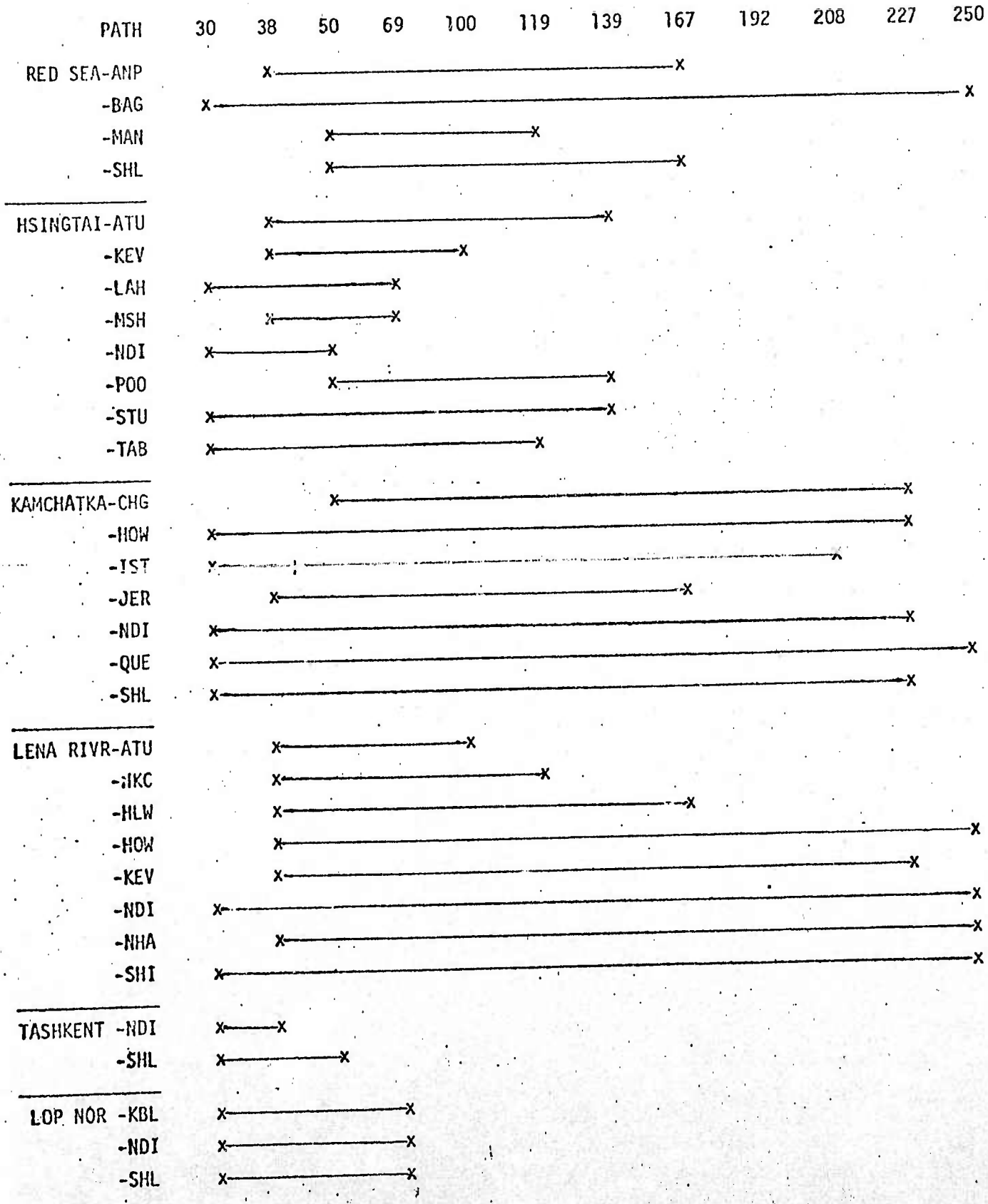
PERIOD RANGE (sec)
PATH
30
38
50
69
100
119
139
167
192
208
227
250
RED SEA-ANP
-BAG
-MAN
-SHL
HSINGTAI-ATU
-KEV
-LAH
-MSH
-NDI
-POO
-STU
-TAB
KAMCHATKA-CHG
-HOW
-IST
-JER
-NDI
-QUE
-SHL
LENA RIVR-ATU
-IKC
-HLW
-HOW
-KEV
-NDI
-NHA
-SHI
TASHKENT -NDI
-SHL
LOP NOR -KBL
-NDI
-SHL

geophysical provinces, as expected from surface wave studies, are to be found. The regions we have used are

1. Ancient PreCambrian Shields
2. Younger (seismically) Stable Platforms
3. The Himalayan-Alpide Mountain Belt
4. The Tibetan Plateau
5. The Sinkiang-Mongolian Seismic Zone
6. The Chinese "Stable" Region

The ancient PreCambrian Shields are well-defined, both as tectonic (from the map) and seismic units. The same comments apply to the Younger Stable Regions. Although few seismic data have been accumulated to date with regard to folded mountain belts -- the exception is the Alps (Knopoff et al.,1966) -- for convenience in computation, we establish this zone as a single seismic province. Region 4, the Tibetan Plateau, is definable in terms of the enormous elevation associated with this region. We have no justification for setting up regions 5 and 6, except that these seem to be regions definable in terms of seismic activity; the modern seismic activity of these regions is inconsistent with surface geology (very old rocks, in some cases) and to us indicates the presence of some anomalous behavior in the upper mantle. Although these regions, within themselves, encompass widely differing geologic structures and widely varying seismic activity, we have assumed that each of these regions is homogeneous. In the inversion, we have not assumed a priori that these two regions have a structure which is similar to that of any of the other numbered regions; should the inversion give the result that regions 5 and 6 are the same as one of the other regions, this can be used to simplify the inversion in a later stage. It can be seen from the table of period ranges of the

observations that the inability to obtain long-period information, from the observations of the Tashkent earthquake and the Lop Nor nuclear explosion, limits our ability to resolve deeper structure under region 4. This will be more evident in the results of the inversion to be described below.

Two small regions are not included in our inversion: The South China Sea, and the Sea of Okhotsk. For the South China Sea, we have assumed the structure to be known, and to be that for typical marginal seas. The phase delays for this region are taken from two single-station phase velocity observations in marginal seas obtained by Leeds (1973) and from two phase velocity determinations by the two-station method obtained by Knopoff (unpublished) across the Philippine Sea. Phase velocity corrections for the Sea of Okhotsk were obtained theoretically from a structure derived from Kosminskaya et al. (1969), in which the Okhotsk depression has a 25 km crustal structure; we have used an oceanic mantle below this crust. These phase corrections have been applied to travel times for those paths that traverse these two regions.

The total path length summed over all event-paths in each region is given in the following table:

TABLE 2

Region	Path Length (km)	Percentage of Total Path Length	Weighted Percentage of Total Path Length
1	20970	12.1	13.0
2	53150	30.6	30.4
3	38411	22.1	22.5
4	15292	8.8	6.9
5	35994	20.7	20.7
6	9979	5.7	6.5
TOTAL	173796	100.0	100.0

Since the harmonic analysis for phase has not been carried out over the same band of periods, a column of the above table has been included to give the product of path length by number of period estimates of phase. By either method of estimation, the very low fraction of sampling in regions 4 and 6 will give us large uncertainties in the structure obtained from the inversion for these regions.

We have inverted the data under the assumption that a simple ray theory for surface waves applies. That is, the phase shift for a seismic wave passing through a given region is computed as though that region were laterally infinite in extent and uninfluenced by the presence of neighboring regions, no matter how close the great circle path approaches the regional boundaries. This assumption is evidently untenable but provides a basis for starting an inversion; future work is planned to test the accuracy of this assumption and to provide a means of approximate correction.

The inversion proceeds as in the method described by Leeds et al. (1974). We calculate the phase travel time for the n^{th} path and the p^{th} period as

$$t_{np} = \sum_{i=1}^{6} \ell_{in} s_{ip}$$

where ℓ_{in} is the path length of the n^{th} path in the i^{th} region ($i=1,\ldots,6$) and s_{ip} is the (theoretical) phase slowness for the i^{th} region at the p^{th} period. The phase slownesses s_{ip} are functions of the model parameters in each region.

The more model parameters we take in each region, the greater the uncertainties in the determination of the parameters. We minimize

$$\sum_n \sum_p (t_{np_0} - t_{np})^2$$

where t_{np_0} is the observed travel-time for the n^{th} path at the p^{th} period. The minimization takes place with respect to the choice of model parameters.

The inversion becomes less and less accurate, i.e., we obtain large variances in the model parameters, as the number of model parameters increases. It would be pleasing to be able to solve for the properties of the crust in each of the six regions. However, this a) requires much precise data at periods shorter than 30 sec., b) increases the number of model parameters significantly, and c) undoubtedly pushes our postulate of lateral homogeneity in each of the regions to an untenable extreme. We have therefore used model crusts for each of the regions which a) seem to be plausible when compared with results for other similar parts of the earth where observations exist (such as locations typical of regions 1, 2 and 3), and b) agree with Soviet refraction data when available. When large residuals were encountered at short periods, such as in the case of region 3 (Alpide-Himalayan belt) and region 4 (Tibetan plateau), we were obliged to introduce more low-velocity material into the crust. This was done by keeping crustal velocities fixed and increasing crustal thickness. In these two cases, this procedure leads to extraordinarily thick crusts. It should be realized that these

model crustal thicknesses are consequences of the procedures used; if we had chosen to lower the crustal velocities, the thicknesses would have been less.

We have parameterized the mantle into a lid, channel and subchannel; each of these layers in a given region is homogeneous. The subchannel region terminates at a depth of 420 km. Below this depth, we place a standard lower mantle platform under all regions. Once again, in order to reduce the number of degrees of freedom in the inversion, we have fixed the lid S-wave velocity at 4.65 km/sec and the subchannel S-wave velocity at 4.8 km/sec. The value of 4.65 km/sec for the lid was chosen because it arises frequently in inversions for many other parts of the world. In the most obvious case in which a 4.65 km/sec lid was not observed, namely for the Western United States (Biswas and Knopoff,1974) in which the subcrustal material has S-wave velocity around 4.3 km/sec, we can assume that a model with a 4.65 km/sec lid with zero lid thickness was accepted by the inversion and that the 4.3 km/sec value is representative of channel material rising almost to the crust. Should the lid velocity in some region be less than 4.65 km/sec in reality, then crustal thicknesses can be reduced; we suspect that for regions 3 and 4 this possibility may exist. A similar comment can be made about the subchannel velocity: if the subchannel velocity should turn out to be less than 4.8 km/sec in some regions, channel thicknesses will be reduced.

The parameterization thus includes only two adjustable model parameters for each region. These are the lid thickness

and the channel S-wave velocity. A thirteenth parameter is the subchannel thickness, which is presumed to be uniform across the entire continent and hence has the same value under each region. Since the crustal thickness and the depth to the 420 km interface are fixed, the parameterization of lid and subchannel thicknesses is equivalent to a parameterization of the depth below the surface of the top and bottom of the channel. This parameterization has 13 degrees of freedom.

After adjustment of the crust by the procedures described above (with interpretation of crustal parameters according to the caveats expressed above), the parameterization and cross-sections used in a linearized inversion procedure are given in Table 3. The superficial sedimentary layer that is introduced in the crusts of regions 3 and 4 is designed to reduce the residuals at the shortest periods.

TABLE 3

Model parameters for inversion of phase velocity data

	Thickness	Depth	β(km/sec)	α(km/sec)	ρ(gm/cm³)
		0			
CRUST	(different crustal models for each region)				
		(fixed)			
LID	VAR		4.65	8.17	3.45
CHANNEL			VAR	7.80	3.45
SUBCHANNEL	VAR		4.80	8.80	3.65
		420(fixed)			
	94		5.128	9.609	3.806
		514			
	94		5.283	9.781	3.934
		608			
	63		5.419	9.902	4.051
		691			
	138		6.172	10.552	4.417
		809			
	139		6.266	11.238	4.505
		948			
	104		6.351	11.392	4.579
		1052			

TABLE 3 (cont'd)

Detailed Crustal Models Used in Inversion

(thickness in km, velocities in km/sec, density in gm/cm^3)

Region 1

h	β	α	ρ
5	3.49	6.05	2.75
20	3.67	6.35	2.85
20	3.85	7.05	3.08

crustal thickness = 45

Region 2

h	β	α	ρ
5	3.49	6.05	2.75
35	3.67	6.35	2.80
5	3.85	7.05	3.08

crustal thickness = 45

Region 3

h	β	α	ρ
2	2.55	4.41	2.41
35	3.5	6.06	2.70
28	3.67	6.35	2.80

crustal thickness = 65

Region 4

h	β	α	ρ
6	2.55	4.41	2.41
26	3.45	5.97	2.70
22	3.67	6.35	2.85
23	3.85	7.05	3.08

crustal thickness = 77

Region 5

h	β	α	ρ
30	3.49	6.05	2.75
15	3.67	6.35	2.80

crustal thickness = 45

Region 6

h	β	α	ρ
10	3.49	6.05	2.75
35	3.67	6.35	2.80

crustal thickness = 45

The starting set of thirteen parameter in the linearized inverse is (in the usual units):

TABLE 4

Region	β_{CH}	h_{LID}	h_{SUB}	Depth to top of channel	Depth to bottom of channel
1	4.51	110	↑	155	↑
2	4.39	113		158	
3	4.30	54	150	119	270
4	4.29	90		167	
5	4.08	92		137	
6	4.38	103	↓	148	↓

The thirteen parameters in the rectangular box in Table 4 are those varied in the inversion.

The accuracies of the measurements were taken to be the same as those used by Leeds et al. (1974), namely a measurement error presumed to be 7 sec for periods less than 70 sec and one-tenth the period for periods greater than 70 sec (hence, at a period of 357 sec, the presumed standard error is 36 sec).

In the inversion, an iteration process has been used in which the matrix of partial derivatives G was recalculated whenever we moved into a new portion of parameter space. This process was continued until we obtained satisfactory convergence of the variable model parameters. The thirteen eigenvalues to the product matrix of partial derivatives G^TG, which were obtained in the final stage of the iteration process, are

given in Table 5. Each eigenvalue corresponds to an eigenvector which in every case points in a direction close to one of the thirteen parametric axes. Thus, each eigenvector can be said to be a discriminant for one of the thirteen degrees of freedom in the model. From the theory of the inversion analysis, we know that the eigenvectors corresponding to the largest eigenvalues give reliable structural information concerning the model parameters closest to them, and that the eigenvector corresponding to the smallest eigenvalue gives little information about its corresponding model parameter.

TABLE 5

	Eigenvalue	Model parameter most closely resolved by eigenvector
1.	13.68	β_{CH2}
2.	8.43	β_{CH5}
3.	6.85	β_{CH3}
4.	3.56	β_{CH1}
5.	2.87	$\beta_{CH6} + h_{SUB}$
6.	2.59	$\beta_{CH6} + h_{SUB}$
7.	1.84	β_{CH4}
8.	1.61	h_{LID5}
9.	1.14	h_{LID2}
10.	1.04	h_{LID3}
11.	0.56	h_{LID6}
12.	0.36	h_{LID1}
13.	0.21	h_{LID4}

From this table, it can be seen that in general the data contain the greatest amount of information about the channel velocities and the least information about the lid thicknesses. In general, the data contain more information about regions 2, 3 and 5 than the other three regions. This is due to the higher percentage of total path length which samples regions 2, 3 and 5. (For complete details, see Table 2 and Fig. 24).

The variance of each model parameter decreases as successive models approach the final one, which demonstrates the convergence of our inversion procedure. Fig. 25 gives our final results: the best model (in a "least-squares" sense) and the corresponding standard deviations of each model parameter. The quality of the agreement of our model to the experimental data is expressed by the parameter R :

$$R = \left[\frac{1}{n} \sum_{i=1}^{n} (\Delta t_i / \sigma_i)^2 \right]^{1/2}$$

where n is the total number of observations, Δt_i is the travel time residual and σ_i is the presumed standard error in the data. If the error for each observation has been correctly estimated, R should be about 1.0 for the final model. A value of $R<1$ suggests that the errors are smaller than estimated; $R>>1$ indicates a poorly-fitting model. The value of R is 1.126 for the final model from our inversion.

From Fig. 25, we also see that the upper mantle structure for regions I and II are very similar. The lid in region I is somewhat thicker. The channel shear-wave velocity for region I

is slightly less than that in region II, but the uncertainty of the model parameter in region I is rather large; thus, the existence of a low-velocity channel in region I is uncertain. The most striking result of this inversion is the very thin lid, and moderate shear-wave velocity, in the channel for region III and V. These two regions exhibit tectonic activity and high seismicity. Region IV is that in which the Eurasian and Indian continents are in collision. Although the upper mantle structure for this region appears to be very similar to those of regions I and II, the uncertainties in the model parameters are large. This is due 1) to the low percentage of total path length in this region, and 2) to the fact that most of the paths which sample this region have only short-period information. Region VI has a thick lid and a pronounced low-velocity channel, but the standard deviations are rather large; additional paths will be required to improve the resolution of the structural parameters in this region.

A number of control experiments and additional measurements are planned for our next contract. These include:

1) Acquisition of additional, longer-period phase velocity information which samples the regions not well-resolved in our current inversion. These regions include Tibet and Southeastern China.
2) Investigating the stability of the results by varying the location of the provincial boundaries. Some of this work has already been done, but more needs to be done in this regard.
3) Investigating the corrections to the raw data to be applied

to take into account events whose geometrical paths are close to and parallel to provincial boundaries.

4) Seeing whether it is possible to reduce the number of degrees of freedom still further beyond those already considered, possibly by reducing the number of provinces, and by constraining the bottom of the lid to fit the melting curve for peridotite.

5) To acquire Love wave data plus SRO and high-gain data for this region. The SRO data will be especially valuable in helping us to resolve the deeper structure in these regions.

6) Investigating the linearity of the solution by varying the starting model.

Arctic Study. We have measured fundamental mode Rayleigh waves over a number of paths crossing the Arctic Ocean. We have used as sources four earthquakes whose focal parameters are:

Lena River	Aug. 25, 1964	13:47:20.6	78.2°N	126.6°E
Eastern Aleutians(1)	Feb. 6, 1965	01:40:33.2	53.2°N	161.9°W
Eastern Aleutians(2)	Feb. 6, 1965	16:50:23.6	53.3°N	161.8°W
Western Aleutians	Feb. 6, 1965	04:02:53	52.1°N	175.7°E

For each of these earthquakes we have obtained initial phases either from the fault plane solution or from the radiation pattern for Rayleigh waves (as in the case of the Lena River discussed above). We have obtained phase velocities by the single-station method for seven paths crossing the Arctic over the period range 50 to 200 sec. The paths are shown in Figure 26 .

It can be seen that none of these are purely oceanic paths. The heavy line outlines our estimate of the boundary between the continental shelf and the deep ocean basins. The fraction of the geometrical path that each event has in the oceanic part is as follows:

Event	Total path length	Oceanic length	Fraction oceanic
1. Lena - ESK	4816 km	1904 km	.40
2. Lena - KTG	3386	1823	.54
3. East Aleut(1) - KON	7483	4603	.62
4. East Aleut(1) - KTG	5933	916	.15
5. East Aleut(2) - KEV	6347	2334	.37
6. East Aleut(2) - ESK	7818	2714	.35
7. West Aleut. - KEV	6263	844	.13

To reduce the available data to information regarding purely oceanic events, we have decided to use the phase velocity data for the Lena River event recorded at KEV (see discussion above for Eurasia) as a typical continental value and to subtract these numbers, for the appropriate path length contribution, from the phase delays observed for the above 7 path-events. Unfortunately, the two events East Aleut.(1) - KTG and West Aleut.-KEV have such small parts of this total path that are oceanic that we are subtracting two numbers of comparable size and the result is quite unstable. The unreliability of the reduction results for these two cases has obliged us to exclude them from our data set. Accordingly, we have investigated the implications of the phase velocity results for the five remaining paths. The relevant data are given in the following Table:

(Pure) Oceanic Phase Velocities (km/sec)

T(sec)	Lena-ESK	Lena-KTG	E.Al(1)-KON	E.Al(2)-KEV	E.Al(2)-ESK
208	4.64	(4.83)	4.62	4.55	4.52
192	4.52	(4.61)	4.51	4.42	4.42
167	4.38	4.32	4.38	4.22	4.28
139	4.21	4.14	4.24	4.09	4.15
119	4.08	4.06	4.12	4.04	4.11
100	4.01	3.99	4.08	3.96	4.07
69	3.95	3.90	4.00	3.91	4.00
50	3.91	3.82	3.98	3.89	3.92

With so few data, we have not been able to regionalize the

the deep Arctic. The best we can do is consider the deep Arctic as a single province and investigate the consequences of inverting an "average" phase velocity for the region. The average phase velocity is obtained from the above table by weighting by the oceanic path length in each case. The result is (omitting the quantities in parentheses):

T(sec)	c(km/sec)
208	4.59
192	4.47
167	4.32
139	4.18
119	4.10
100	4.03
69	3.97
50	3.92

These results can be compared with those obtained for Pacific paths by Leeds (1973) from inversion of trans-Pacific phase velocity data by methods similar to those described above for trans-Eurasian paths. After inversion and determination of the pure-age cross-sections, the pure-age phase velocities for the Pacific and be derived; these are shown in Fig.27 for Pacific ages 0-10 my, 20-40 my, 85-110my. The Arctic data points are shown as circles. The Arctic cross-section averages out to about a 30 my Pacific structure. According to the model of Parker and Oldenburg (1973), the lithospheric thickness is a function of the age $z(t) = 9.4t^{1/2}$ km , with t the age in my. Thus, assuming that the lid and channel velocities are of the same order as in the Pacific, the age at which the Arctic began to open is calculated to be about 70 my (before present), an unexpectedly small quantity.

Theoretical seismograms. Prior to the availability of the final regionalization from the first part of our investigation, the thrust of our work with time series synthesis has been directed toward improving the efficiency of existing computational techniques. This improvement is required to permit us to extend the information contained on the theoretical seismograms down through the period range covered by the long-period instruments of the WWSSN. Although up to the present time we have concentrated on laterally homogeneous structures, in all other respects our models of the earth have been highly realistic: approximately 200 layers were used to model the radial heterogeneity of the crust-mantle system of a spherical earth, and the intrinsic anelasticity was handled in an exact manner.

A summary of the general methods we have applied in our computations is given by Kausel and Schwab (1973) and Knopoff et al. (1973). An elaboration of, and certain justifications for, these procedures have recently been given by Schwab and Kausel (1976). A recent contribution by Calcagnile et al. (1976, preprint appended), completed under this contract, is also pertinent here, when only the surface-wave portion of the theoretical seismogram is desired.

Algorithmic development and programming improvements, which were carried out under the present contract, are contained in several appended reprints and preprints: Schwab et al. (1974), Nakanishi et al. (1975), Nakanishi et al. (1976a), and Nakanishi et al. (1976b).

The new work is being, and will to be, carried out under our next contract, and involves our preliminary attempts to compare the computed seismograms with the entire record from long-period instruments of the WWSSN. The initial results of this work are reported by Kausel, Schwab and Mantovani (1976, preprint appended), and by Mantovani et al. (1976a, preprint appended). One further manuscript along these lines (Mantovani et al, 1976b) is approaching completion.

Our further plans with this work involve the addition of more of the higher modes in the seismogram synthesis. Currently, we are using 11 modes; we would like to increase this to 21. Also, we are now ready to make the first approach to the treatment of lateral heterogeneity. This will involve the use of three separate structures: one to model the parameters beneath the epicenter, and to be used in the generation of initial excitation and phases at the source; one structure as an "average" over the propagation path; and a final structure to model that beneath the instrument. Finally, to date we have limited our work with theoretical seismograms to the SH component of motion; we are now interested in extending the treatment to include the P-SV (Rayleigh) components.

The final, practical purpose of our work under this contract -- application of our results to the discrimination problem -- involves comparison of theoretical and experimental seismograms. It is therefore important that we have as accurate a means as possible of obtaining the instrumental constants from the impulse response of the experimental record. These constants then permit us to include, with a minimum of error, the

instrumental response on the theoretical seismogram. Our improved scheme for inversion of the impulse response to obtain the electromagnetic instrument constants, which has been devised under the present contract, is described by Mitchel, Knopoff and Schwab (1975, reprint appended) and by Mitchel (1976, preprint appended).

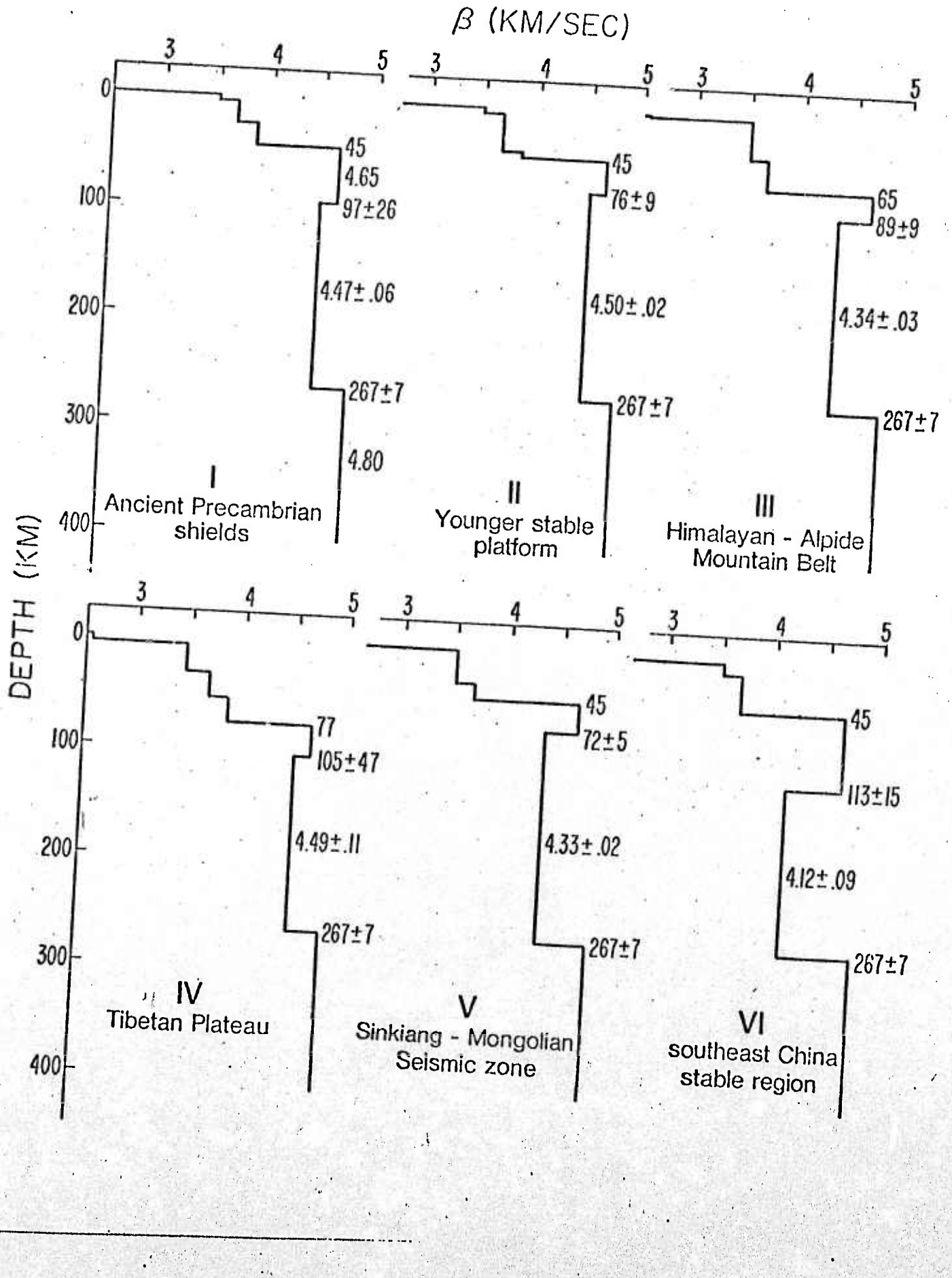
β (KM/SEC)
3
4
5
DEPTH (KM)
0
100
200
300
400
45
4.65
97±26
4.47±.06
267±7
4.80
I
Ancient Precambrian shields
45
76±9
4.50±.02
267±7
II
Younger stable platform
65
89±9
4.34±.03
267±7
III
Himalayan - Alpide Mountain Belt
77
105±47
4.49±.11
267±7
IV
Tibetan Plateau
45
72±5
4.33±.02
267±7
V
Sinkiang - Mongolian Seismic zone
45
113±15
4.12±.09
267±7
VI
southeast China stable region

Fig. 26

Fig. 27

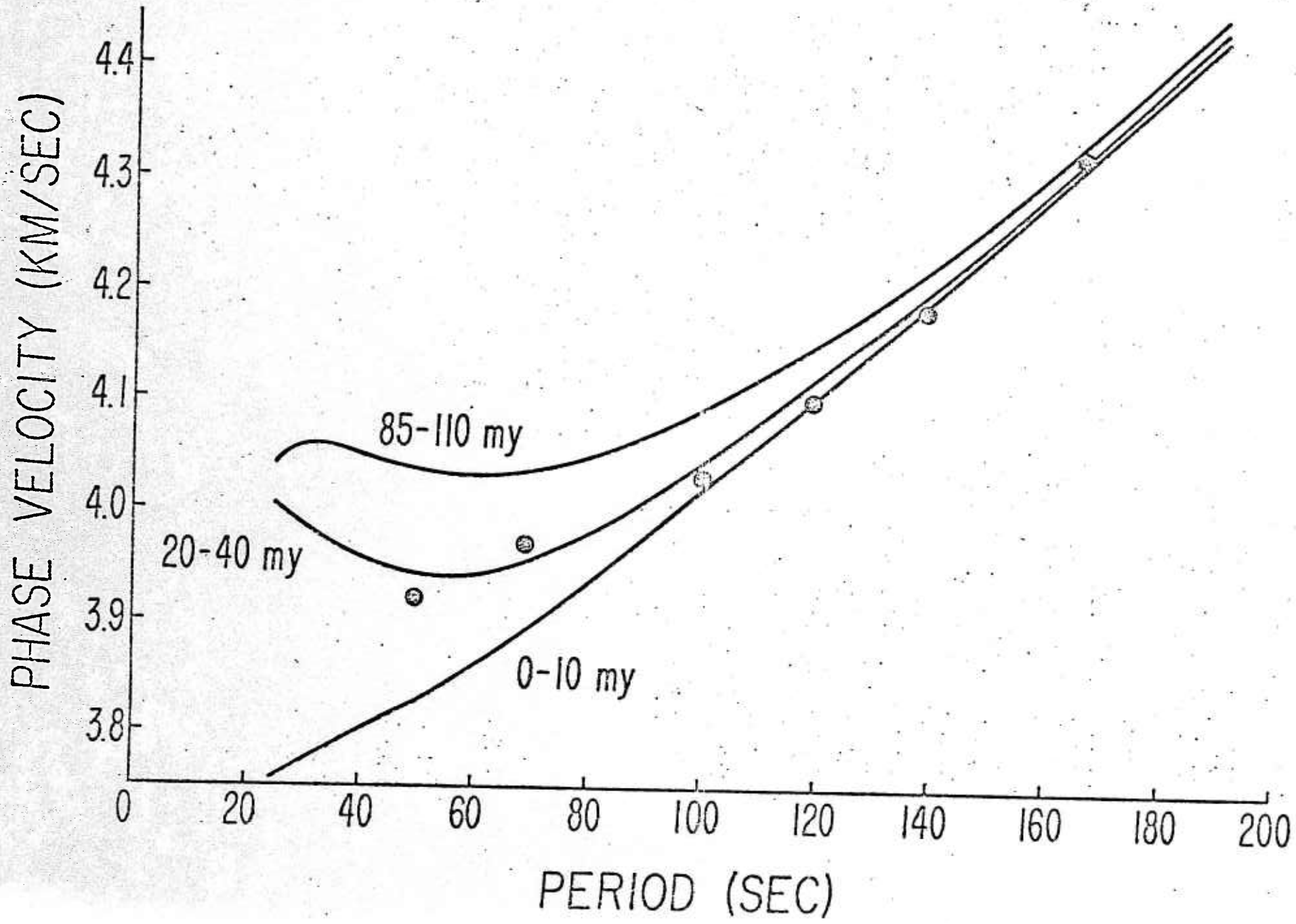
PHASE VELOCITY (KM/SEC)
4.4
4.3
4.2
4.1
4.0
3.9
3.8
85-110 my
20-40 my
0-10 my
0
20
40
60
80
100
120
140
160
180
200
PERIOD (SEC)

Alterman, Z. and D. Loewenthal (1972). Computer generated seismograms, in Methods in Computational Physics, volume 12 (edited by B.A. Bolt), Academic Press, New York, 35-164.

Arkangel'skaya, V.M. (1960). Dispersion of surface waves and crustal structure, Bull. (Izv.) Acad.Sci.USSR, Geophys. Ser. No 9, 904-927.

Ben-Menahem, A. and M.N. Toksöz (1963). Source mechanism from spectra of long-period seismic surface waves. 2. The Kamchatka earthquake of November 4, 1952, J.Geophys.Res., 68, 5207-5222.

Ben-Menahem, A. and D.G. Harkrider (1964). Radiation patterns of seismic surface waves from buried dipolar point sources in a flat stratified earth, J.Geophys.Res., 69 2605-2620.

Biswas, N.N. (1971). The upper mantle structure of the United States from the dispersion of surface waves, Ph.D. thesis, University of California, Los Angeles.

Biswas, N.N. and L. Knopoff (1970). Exact earth-flattening calculation for Love Waves, Bull.Seismol.Soc.Amer., 60, 1123-1137.

Biswas, N.N. and L. Knopoff (1974). Structure of the upper mantle under the United States from the dispersion of Rayleigh waves, Geophys.J.R.astr.Soc., 36, 515-539.

Boore, D.M. (1969). Effect of higher mode contamination on measured Love wave phase velocities, J.Geophys.Res., 74, 6612-6616.

Brune, J., J. Nafe and J. Oliver (1960). A simplified method for the analysis and synthesis of dispersed wave trains, J.Geophys.Res., 65, 287-305.

Burridge, R. and L. Knopoff (1964). Body force equivalents for seismic dislocations, Bull.Seismol.Soc.Amer., 54, 1875-1888.

Calcagnile, G., G.F. Panza, F. Schwab and E.G. Kausel (1976). On the computation of theoretical seismograms for multimode surface waves, submitted to Geophys.J.R.astr.Soc.

Dorman, J. and M. Ewing (1962). Numerical inversion of surface wave dispersion data and the crust-mantle structure in the New York-Pennsylvania area, J.Geophys.Res., 67, 5227-5241.

Fouda, A.A. (1973). The upper mantle structure under the stable regions, Ph.D. thesis, University of California, Los Angeles.

Frez, J. and F. Schwab (1976). Structural dependence of the apparent initial phase of Rayleigh waves, Geophys.J.R. astr.Soc., 44, in press.

Gilbert, F. and A.M. Dziewonski (1975). An application of normal mode theory to the retrieval of structure parameters and source mechanisms from seismic spectra, Phil.Trans.Roy. Soc.London, Ser.A, 278, 187-269.

Haskell, N.A. (1953). The dispersion of surface waves on multilayered media, Bull.Seismol.Soc.Amer., 43, 17-34.

Harkrider, D.G. (1964). Surface waves in multilayered elastic media. Part I. Rayleigh and Love waves from buried sources in a multilayered elastic half-space, Bull. Seismol.Soc.Amer., 54, 627-679.

Harkrider, D.G. (1970). Surface waves in multilayered elastic media. Part II. Higher mode spectra and spectral ratios from point sources in plane layered earth models, Bull. Seismol.Soc.Amer., 60, 1937-1987.

Jackson, D.D. (1972). Interpretation of inaccurate, insufficient and inconsistent data, Geophys.J., 28, 97-109.

James, D.E. and A.T. Linde (1971). A source of major error in the digital analysis of World Wide Standard Station seismograms, Bull.Seismol.Soc.Amer., 61, 723-728.

Kausel, E.G. (1972). Regionalization of the lithosphere and asthenosphere of the Pacific Ocean, Ph.D. thesis, Columbia University, New York.

Kausel, E. and F. Schwab (1973). Contributions to Love wave transformation theory: Earth-flattening transformation for Love waves from a point source in a sphere, Bull. Seismol.Soc.Amer., 63, 983-993.

Kausel, E.G., A.R. Leeds and L. Knopoff (1971). Rayleigh wave phase velocities across the Pacific, Science, 186, 139-141.

Kausel, E.G., F. Schwab and E. Mantovani (1976). Oceanic Sa, in preparation.

Keilis-Borok, V.I. and T.B. Yanovskaya (1967). Inverse seismic problems (structural review), Geophys.J., 13, 223-233.

Khain, V.E. and M.V. Muratov (1969). Crustal movements and tectonic structure of continents, in The Earth's Crust and Upper Mantle, (edited by P.J. Hart), Geophysical Monograph 13, American Geophysical Union, Washington, DC.

Knopoff, L. (1961). Green's function for eigenvalue problems and the inversion of Love wave dispersion data, Geophys.J., 4, 161-173.

Knopoff, L. (1962). Higher order Born approximation for the inversion of Love wave dispersion, Geophys.J., 7, 149-157.

Knopoff, L. (1964). A matrix method for elastic wave problems, Bull.Seismol.Soc.Amer., 54, 431-438.

Knopoff, L. (1969). Phase and group slownesses in inhomogeneous media, J.Geophys.Res., 74, 1701.

Knopoff, L. (1972). Observation and inversion of surface wave dispersion, Tectonophysics, 13, 497-519.

Knopoff, L. and F. Schwab (1968). Apparent initial phase of a source of Rayleigh waves, J.Geophys.Res., 73, 755-760.

Knopoff, L. and J.W. Schlue (1972). Rayleigh wave phase velocities for the path Addis Ababa-Nairobi, Tectonophysics, 15, 157-163.

Knopoff, L., F. Schwab and E. Kausel (1973). Interpretation of Lg, Geophys.J.R.astr.Soc., 33, 389-404.

Knopoff, L. and A.A. Fouda (1975). Upper mantle structure under the Arabian Peninsula, Tectonophysics, 26, 121-134.

Knopoff, L., F. Schwab, K. Nakanishi and F. Chang (1974). Evaluation of Lg as a discriminant among different continental crustal structures, Geophys.J.R.astr.Soc., 39, 41-70.

Kosminskaya, I.P. and Yu.V. Riznichenko (1964). in the earth's crust in Eurasia, in Research in Geophysics, volume 2 (edited by H. Odishaw) MIT Press, Cambridge.

Kosminskaya, I.P., N.A. Belyaevsky and I.S. Volvovsky (1969). Explosion seismology in the USSR, in The Earth's Crust and Upper Mantle, (edited by P.J. Hart), Geophysical Monograph 13, American Geophysical Union, Washington, DC.

Leeds, A.R. (1973). Rayleigh wave dispersion in the Pacific Basin, Ph.D. thesis, University of California, Los Angeles.

Leeds, A.R. (1975). Lithospheric thickness in the Western Pacific, Phys.Earth Planet.Int., 11, 61-64.

Leeds, A.R., L. Knopoff and E.G. Kausel (1974). Variations of upper mantle structure under the Pacific Ocean, Science, 186, 141-143.

Lubimova, E.A. and B.G. Polyak (1969). Heat flow map of Eurasia, in The Earth's Crust and Upper Mantle (edited by P.J. Hart), Geophysical Monograph 13, American Geophysical Union, Washington, DC.

Mantovani, E., F. Schwab, H. Liao and L. Knopoff (1976a). Generation of complete theoretical seismograms for SH. II. Eleven modes in an oceanic structure, submitted, Geophys. J.R.astr.Soc.

Mantovani, E., F. Schwab, L. Knopoff and H. Liao (1976b). Interpretation of oceanic Sn, in preparation.

Maruyama, T. (1963). On the force equivalents of dynamical elastic dislocations with reference to the earthquake mechanism, Bull.Earthq.Res.Inst., 41, 467-486.

Mitchel, R., L. Knopoff and F. Schwab (1975). Improved scheme of inversion of seismometer impulse response to obtain electromagnetic instrument constants, Earthq.Notes (Eastern Section Seismol.Soc.Amer.) 46, no. 3, 41.

Molnar, P., J. Savino, L.R. Sykes, R.C. Liebermann, G. Hade and P.W. Pomeroy (1969). Small earthquakes and explosions in Western North America recorded by new high gain, long period seismographs, Nature, 224, 1268-1273.

Nakanishi, K., F. Schwab, L. Knopoff and E. Mantovani (1975). Generation of complete SH theoretical seismograms (abstract), Transactions Amer.Geophys.Union, 56, 1026-1027.

Nakanishi, K., F. Schwab and L.G. Kausel (1976a). Interpretation of Sa in a continental structure, Geophys.J.R.astr.Soc., in press.

Nakanishi, K., F. Schwab and L. Knopoff (1976b). Generation of complete theoretical seismograms for SH. Part I. Eight modes in a continental structure, submitted to Geophys.J.R.astr.Soc.

Parker, A.C. and D.E. Oldenburg (1973). Thermal model of ocean ridges, Nature Physical Science, 242, 137-139.

Pilant, W.L. and L. Knopoff (1970). Inversion of phase and group slowness dispersion, J.Geophys.Res., 75, 2135-2136,

Pomeroy, P.W., G. Hade, J. Savino and R. Chander (1969). Preliminary results from high-gain wide-band long-period electromagnetic seismograph systems, J.Geophys.Res., 74, 3295-3298.

Popov, I.I. (1960). Dispersion of long-period Love waves in the continental and oceanic crust along the path Indonesia-Crimea, Bull.(Izv.)Acad.Sci.USSR, Geophys.Ser. No. 10, 970-973.

Press, F. (1968). Earth models obtained by Monte Carlo inversion, J.Geophys.Res., 73, 5223-5233.

Press, F. (1969). The sub-oceanic mantle, Science, 165, 174-176.

Rezanov, I.A. and V.M. Kochetov (1962). Recent tectonics and seismic regionalization in the northeastern region of the USSR, Bull.(Izv.)Acad.Sci.USSR, Geophys.Ser. No 12, 1045-1052.

Saito, M. (1967). Excitation of free oscillations and surface waves by a point source in a vertically heterogeneous earth, J.Geophys.Res., 72, 3689-3699.

Santô, T.A. (1960a). Observations of surface waves by Columbia-type seismograph installed at Tsukuba Station, Japan. (Part I) -- Rayleigh wave dispersions across the oceanic basin, Bull.Earthq.Res.Inst., 38, 219-240.

Santô, T.A. (1960b). Rayleigh wave dispersions across the oceanic basin around Japan (Part II), Bull.Earthq.Res. Inst., 38, 385-401.

oceanic basin around Japan (Part III), Bull.Earthq. Res.Inst., 39, 1-22.

Santô, T.A. (1961b). Division of the Southwestern Pacific area into several regions in each of which Rayleigh waves have the same dispersion characters, Bull.Earthq. Res.Inst., 39, 603-630.

Santô, T. (1962). Dispersion of surface waves along various paths to Uppsala, Sweden. Part I: Continental paths, Annal.Geofis., 15, 245.

Santô, T. (1965a). Lateral variation of Rayleigh wave dispersion character. Part I: Observational data, Pure and Applied Geophys., 62, 49-66.

Santô, T. (1965b). Lateral variation of Rayleigh wave dispersion character. Part II: Eurasia, Pure and Applied Geophys., 62, 67-70.

Satô, Y., T. Usami and M. Landisman (1968). Theoretical seismograms of torsional disturbances excited at a focus within a heterogeneous spherical earth -- Case of a Gutenberg-Bullen earth model, Bull.Seismol.Soc.Amer., 58, 133-170.

Savarensky, E.F. and Sh.S. Ragimov (1958). Determining the velocity of Rayleigh waves and direction to the epicenter by three nearby stations, Bull.(Izv.)Acad.Sci. USSR, Geophys.Ser. No. 12, 866-869.

Savarensky, E.F., O.N. Solov'eva and B.N. Shechkov (1959). Love wave recording at seismological station Moscow and crustal structure, Bull.(Izv.)Acad.Sci.USSR, Geophys. Ser. No. 5.

Savarensky, E.F. and D.I. Sikharulidze (1959). Crustal thickness determinations from measured Love wave dispersion, Bull.(Izv.)Acad.Sci.USSR, Geophys.Ser.No. 6.

Savarensky, E.F. and Sh.S. Ragimov (1959). On the determination of the average thickness of the earth's crust from Rayleigh wave group velocity measurements, Bull.(Izv.)Acad.

Sci.USSR, Geophys.Ser.No. 9, 969-971.

Savarensky, E.G. and B.N. Shechkov (1961). The structure of the earth's crust in Siberia and in the Far East from Love and Rayleigh wave dispersion data, Bull.(Izv.) Acad.Sci.USSR, Geophys.Ser. No. 5, 4540456.

Savarensky, E.F. and A.B. Peshkov (1968). On the use of surface wave velocities in choosing a model of crustal structure, Akad.Nauk SSR Izv., Fizika Zemli No. 10, 79-87.

Savarensky, E.F., G.N. Bozhko, T.I. Kukhtikova, A.B. Peshkov, I.I. Popov, B.N. Sheshkov, O.I. Yurkevich and L.M. Yudakova (1969). On the earth structure in some regions of the USSR from surface wave data, Pure and Applied Geophysics, 73, 99-119.

Savino, J., K. McCamy and G. Hade (1972). Structures in earth noise beyond twenty seconds -- a window for earthquakes, Bull.Seismol.Soc.Amer., 62, 141-176.

Schwab, F. (1970). Surface wave dispersion computations: Knopoff's method, Bull.Seismol.Soc.Amer., 60, 1491-1520.

Schwab, F. and L. Knopoff (1970). Surface wave dispersion computations, Bull.Seismol.Soc.Amer., 60, 321-344.

Schwab, F. and L. Knopoff (1971). Surface waves on multilayered anelastic media, Bull.Seismol.Soc.Amer., 61, 893-912.

Schwab, F. and L. Knopoff (1972). Fast surface wave and free mode computations, Chapter 3, in Methods in Computational Physics, Volume 11 (edited by B.A. Bolt) Academic Press, New York, 87-180.

Schwab, F. and L. Knopoff (1973). Love waves and the torsional free modes of a multilayered anelastic sphere, Bull. Seismol.Soc.Amer., 63, 1107-1117.

Schwab, F., L. Knopoff, K. Nakanishi and E. Kausel (1974). Interpretation of Sa (abstract), Earthq.Notes (Eastern Section Seismol.Soc.Amer.), XLV, No. 2, 12-13.

Schwab, F. and E.G. Kausel (1976). Long-period surface wave seismology: Love wave phase velocity and polar phase shift, Geophys.J.R.astr.Soc., 45, 407-435.

Shechkov, B.N. (1961). Structure of the earth's crust in Eurasia from the dispersion of surface waves, Bull. (Izv.)Acad.Sci.USSR, Geophys.Ser.No. 5, 450-453.

Shechkov, B.N. (1964). Seismic surface wave dispersion and Eurasian crustal structure, Bull.(Izv.)Acad.Sci.USSR, Geophys.Ser. No. 3, 183-187.

Shechkov, B.N. (1970). Surface wave group velocities on Eurasian paths, Akad.Nauk SSR Izv.Fizika Zemli No. 8, 80-87.

Shechkov, B.N. and O.N. Solov'eva (1961). Group velocites of Rayleigh waves traveling along a mixed continental-oceanic path, Bull.(Izv.)Acad.Sci.USSR, Geophys.Ser. No. 8, 768-771.

Sikharulidze, D.I. and R.K. Makharadze (1968). The problem of using surface waves in seismic exploration, Akad.Nauk Gruzin.SSR Soobshch. 52, 335-360.

Sollogub, V.B. (1969). Seismic crustal studies in Southeastern Europe, in The Earth's Crust and Upper Mantle, (edited by P.J. Hart), Geophysical Monograph 13, American Geophysical Union, Washington, DC.

Sykes, L.R. (1967). Mechanism of earthquakes and nature of faulting on the mid-oceanic ridges, J.Geophys.Res., 72, 2131-2153.

Takeuchi, H. and M. Saito (1972). Seismic surface waves, in Methods in Computational Physics, Volume 11 (edited by B.A. Bolt), Academic Press, New York, 217-295.

Thatcher, W. and J.N. Brune (1969). Higher mode interference and observed anomalous apparent Love wave phase velocities, J.Geophys.Res., 74, 6603-6611.

Thomson, W.T. (1950). Transmission of elastic waves through a stratified solid medium, J.Appl.Phys., 21, 89-93.

Wiggins, R.A. (1972). The general linear inverse problem: Implication of surface waves and free oscillations for earth structure, Revs.Geophys. and Space Phys., 10, 251-285.

Zakharova, A.I, L.M. Matasova and O.V. Soboleva (1971) Mechanism of the focus of the main shock from instrumental data, in Tashkent Earthquake of 26 April 1966 (ed. G.A. Mavlyanov) F.A.N. Tashkent Publ. House, Tashkent, USSR, 53-58.

V. Figure Captions

FIG. 1. Locations of WWSSN stations and new, high-gain installations to be used in the investigation.

FIG. 2. Example of the large-magnitude seismicity of the region we propose to study. The regions of high, large-magnitude seismicity along the eastern border of the Kamchatka peninsula and along the Aleutian arc may also provide useful events for the study.

FIG. 3. Limits (solid lines) of the region we propose to cover with a dense set of epicenter-to-station paths. Solid regions are those of high, large magnitude seismicity.

FIG. 4. First-motion information and fault plane solution for event occurring at 21:29:17.4 GMT on March 7, 1966.

FIG. 5. Location of epicenter and epicenter-to-station paths selected for processing from event occurring at 21:29:17.4 GMT on March 7, 1966.

FIG. 6. Geometry and coordinate systems of fault plane, focus, and epicenter.

FIG. 7. Location of epicenter and epicenter-to-station paths selected for processing for event occurring at 13:47:20.6 GMT on August 25, 1964.

FIG. 8. First-motion information to be used for fault-plane solution for event occurring at 13:47:20.6 GMT on August 25, 1964. The solution given by Sykes (1967) is indicated by dotted lines

FIG. 9. Rayleigh-wave amplitude information to be used for fault-plane solution for event occurring at 13:47:20.6 GMT on August 25, 1964. The central set of radiation patterns are the results of theoretical computations based on the fault plane solution given in the text. The other four radiation patterns depict the experimental results.

FIG. 10. Location of epicenter and epicenter-to-station paths selected for processing from event occurring at 14:30:29.1 GMT on December 26, 1964.

FIG. 11. Results from first-motion fault plane analysis for event occurring at 14:30:29.1 GMT on December 26, 1964.

FIG. 12. Location of epicenter and epicenter-to-station paths selected for processing for event occurring at 07:15:54.4 GMT on March 31, 1969.

FIG. 13. Location of epicenters and epicenter-to-station paths selected for processing for events occurring at 01:40:33.2 (dashed lines) and 16:50:29 GMT (solid lines) on February 6, 1965.

FIG. 14. Results from first-motion fault plane analysis for events occurring at 01:40:33.2 (Fig.14a) and 16:50:29 GMT (Fig.14b) on February 6, 1965.

FIG. 15. Location of epicenters and epicenter-to-station paths for events occurring at 09:32:09.3 GMT on February 5, 1965 (dashed line) and at 04:02:53 GMT on February 6, 1965 (solid line).

FIG. 16. Results from first-motion fault plane analysis for events occurring at 09:32:09.3 GMT on February 5, 1965 and at 04:02:53 GMT on February 6, 1965.

FIG. 17. Combined Rayleigh wave propagation paths. Continental results are emphasized here.

FIG. 18. Combined Rayleigh wave propagation paths. Arctic results are emphasized here.

FIG. 19. Sample phase velocity results for the paths noted. The paths are shown in Figures 5 and 7.

FIG. 20. Propagation paths across the Eurasian continent from five earthquakes and one nuclear explosion.

FIG. 21. All Eurasian phase velocities can be sorted into two groups (hatched areas), except for phase velocities POO-2 and SHL-1, which fall between these two groups. Phase velocities for "standard" shield (FLO-GOL), younger stable regions (SHA-LUB) and rift zones (TUC-BOZ) are shown for comparison (Biswas and Knopoff,1974). The global average phase velocities obtained from free-mode observations are also shown (F.M.) (Gilbert and Dziewonski, 1975).

FIG. 22. Propagation paths corresponding to the two phase velocity groups in Fig. 21. The solid line indicates a path with higher phase velocity; the dashed line indicates a path with lower phase velocity.

FIG. 23. Regionalization of the Eurasian continent based on the tectonic map of Khain and Muratov (1969).

FIG. 24. Propagation path in each subregion of the Eurasian continent. The percentage of total path length in each region is shown in Table 2.

FIG 25. Final result of 13 variable parameters in the model and their corresponding standard deviations.

FIG. 26. Seven paths used in single-station study of the Arctic region. "Deep" oceanic region is indicated by hatched area.

FIG. 27. Pure-age phase velocity for the Pacific Ocean, and our experimental results for the Arctic Ocean.

Fig. 1

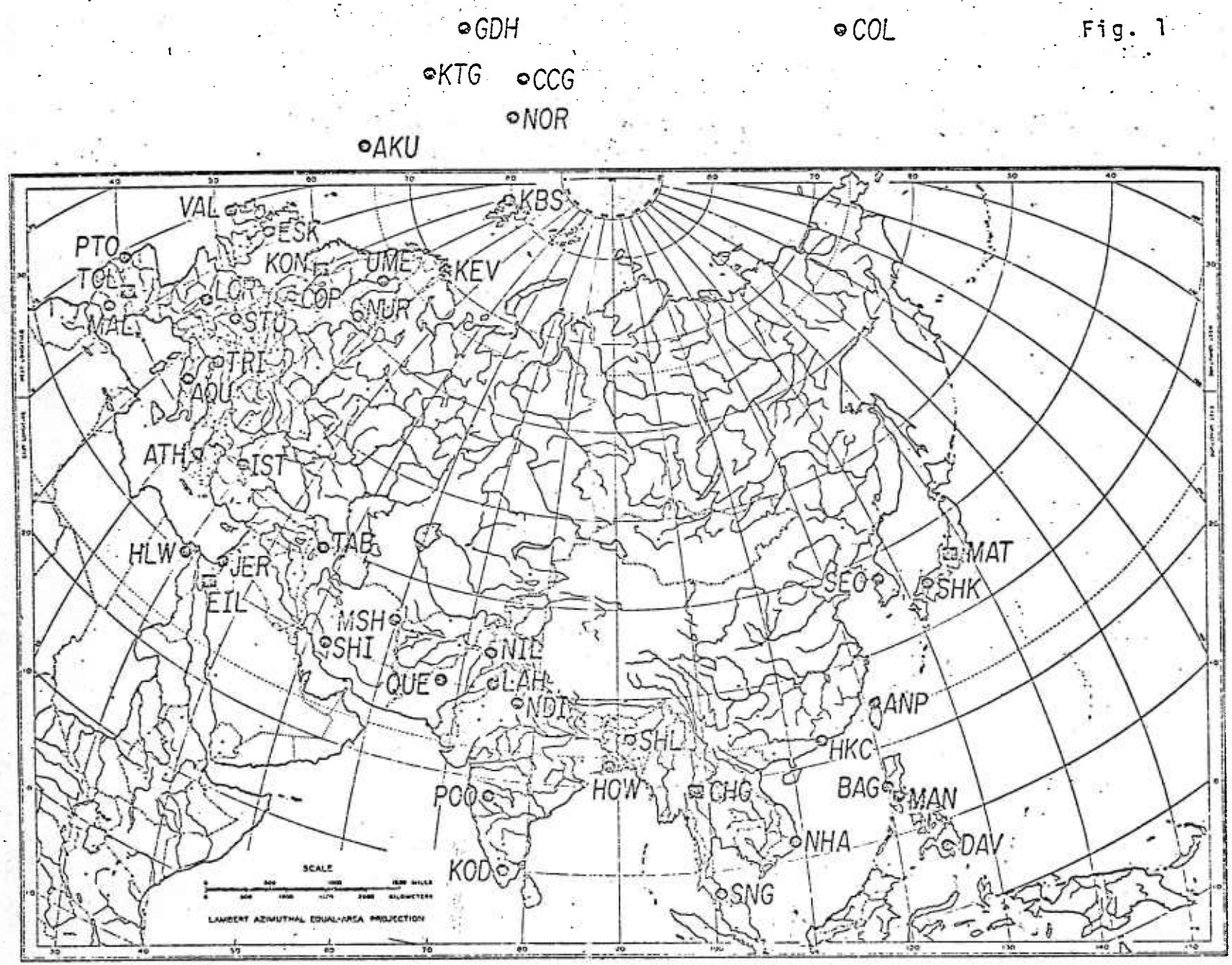

WWSSN STATIONS
HIGH-GAIN, LONG-PERIOD STATIONS

Fig. 2

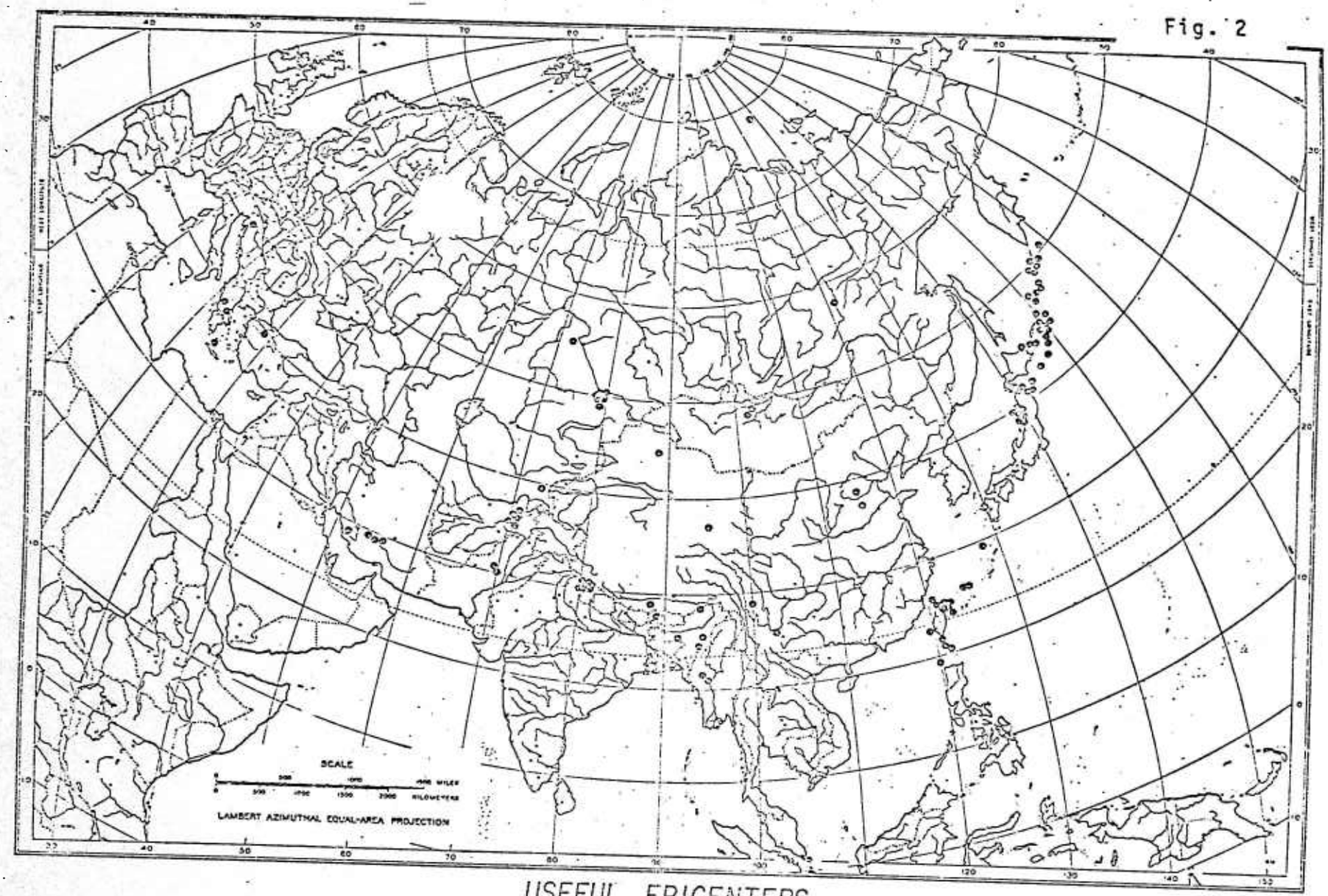

USEFUL EPICENTERS
5.9 ≤ MAGNITUDE ≤ 6.6
FEB. 1963 - FEB. 1967

Fig. 3

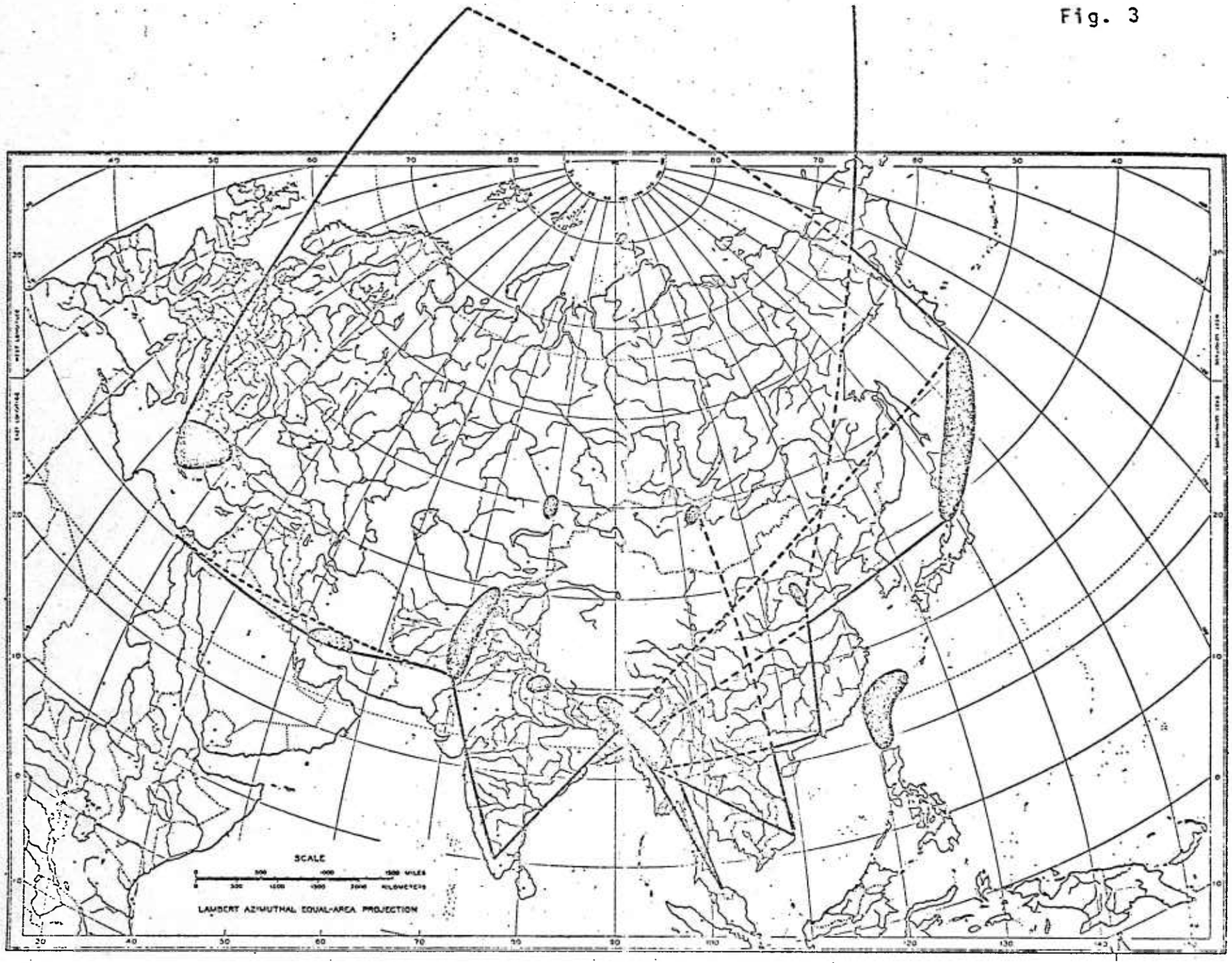

Fig. 4

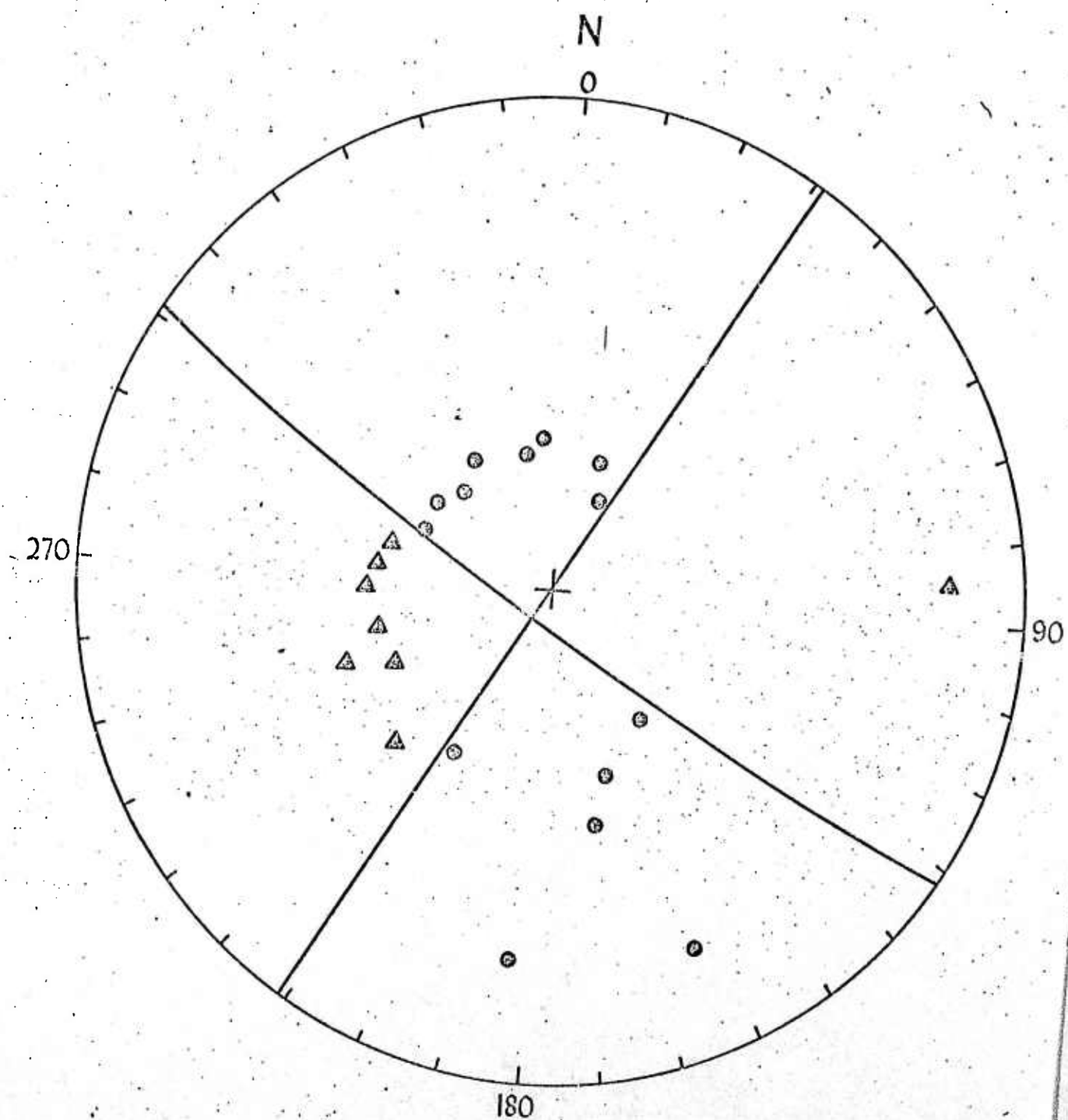

SOURCE DEPTH=15 KM

compression

dilatation

Fig. 5

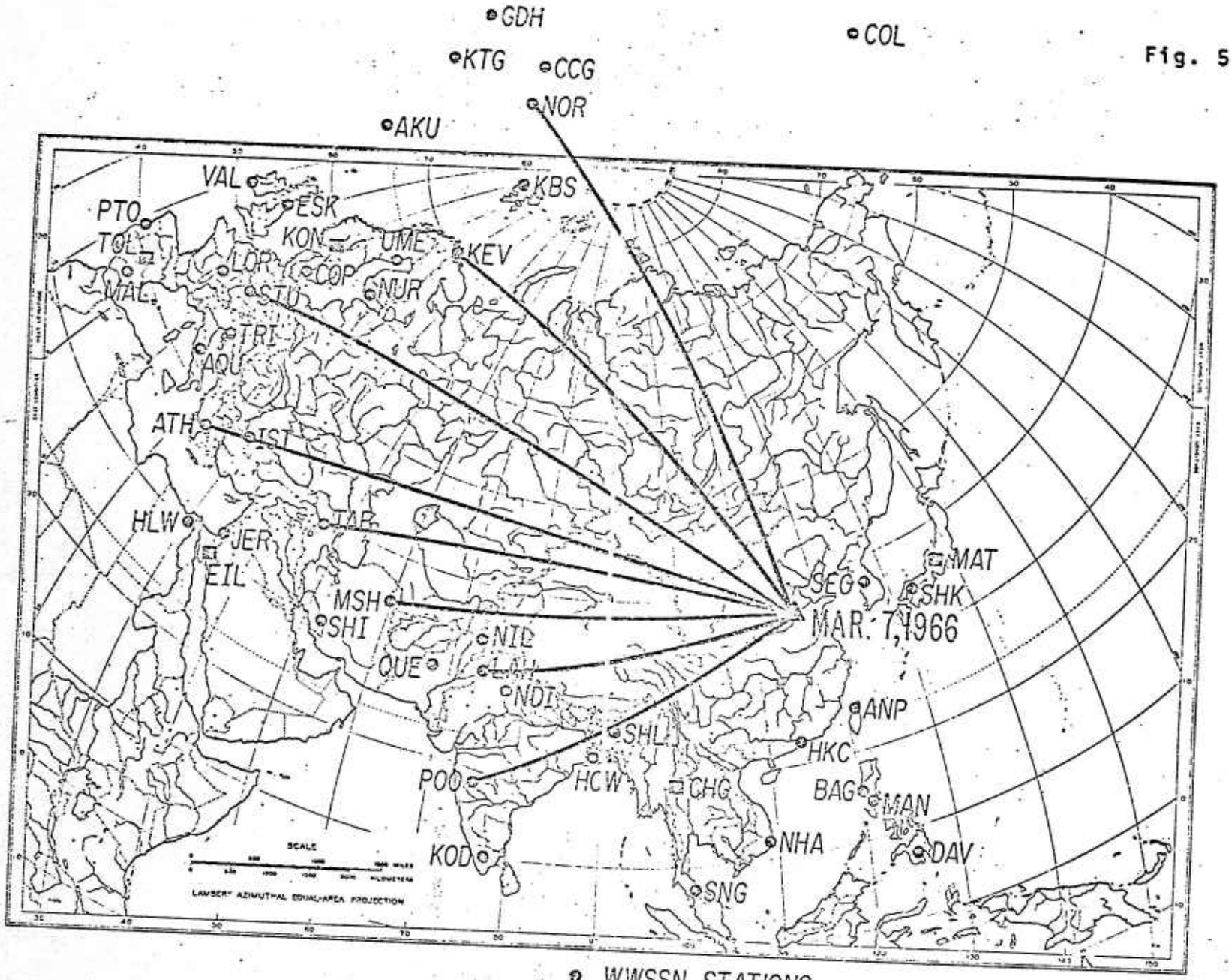

WWSSN STATIONS
HIGH-GAIN, LONG-PERIOD STATIONS

Fig. 6

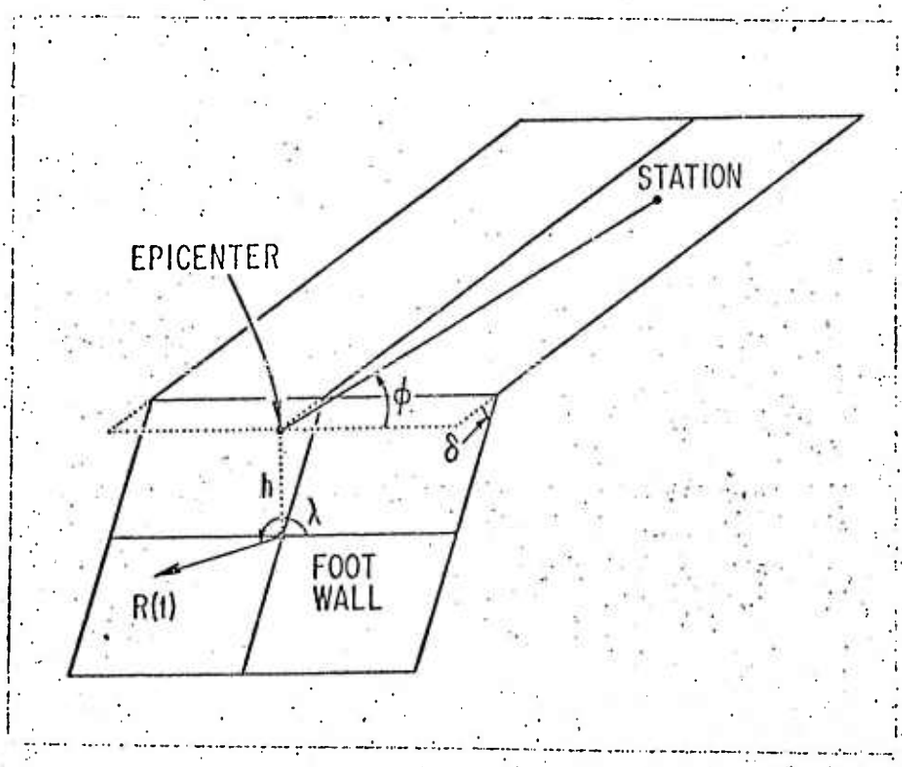

Fig. 7

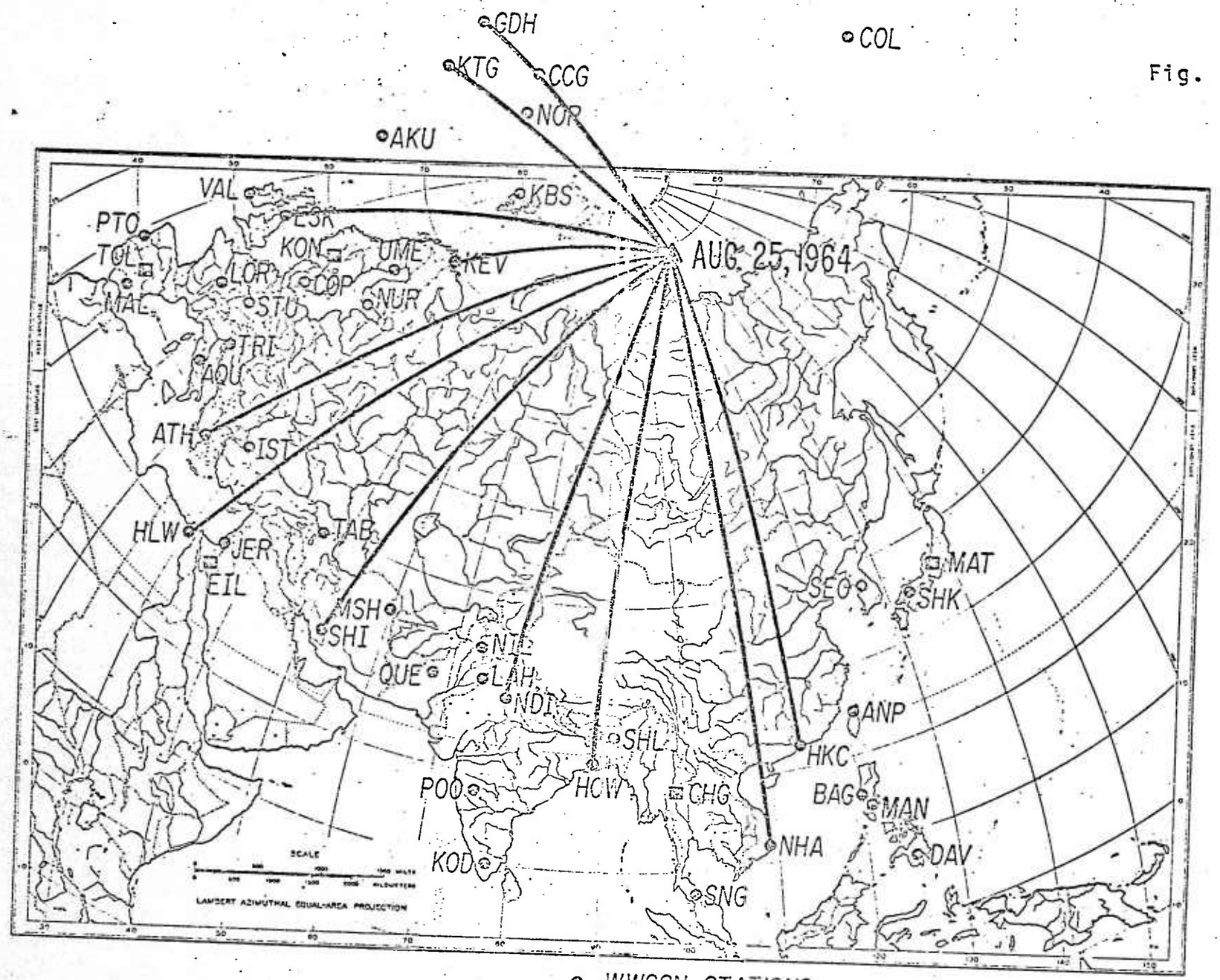

WWSSN STATIONS
HIGH-GAIN, LONG-PERIOD STATIONS

Fig. 8

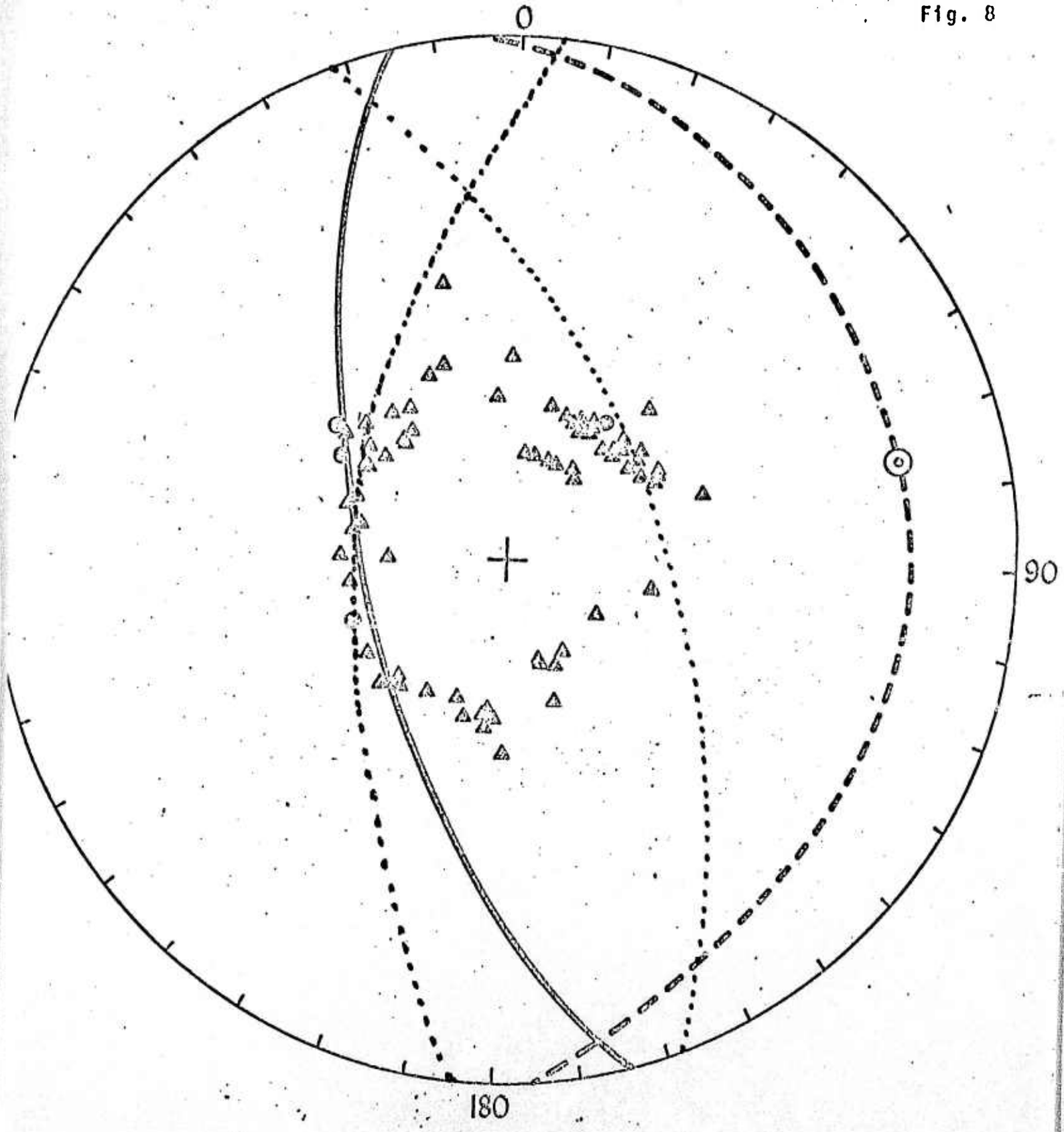

SOURCE DEPTH=11.5 KM

○ compression

△ dilatation

Fig. 9

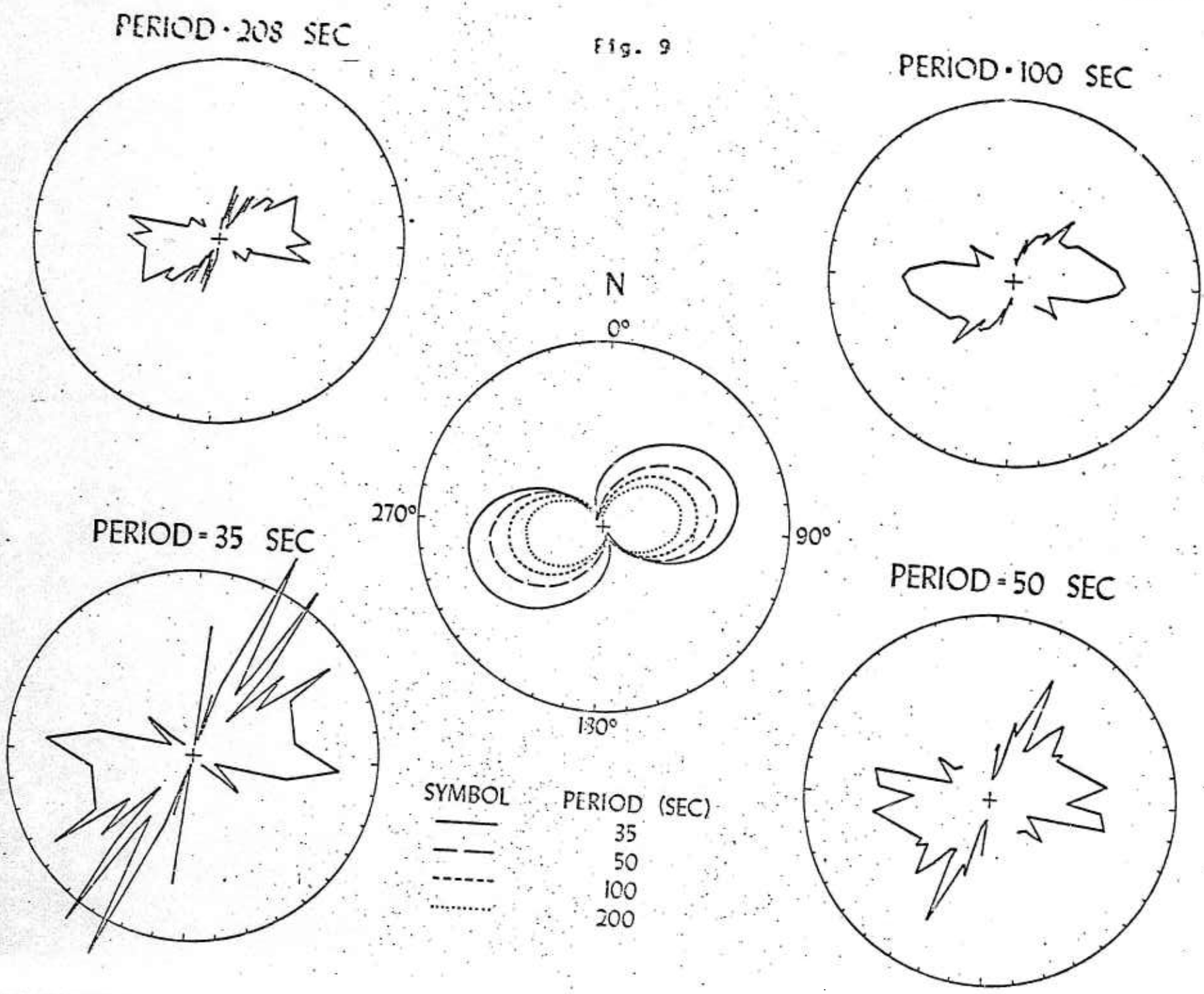
PERIOD · 208 SEC
PERIOD · 100 SEC
N
0°
270°
90°
180°
PERIOD = 35 SEC
PERIOD = 50 SEC
SYMBOL
PERIOD (SEC)
35
50
100
200

Fig. 10

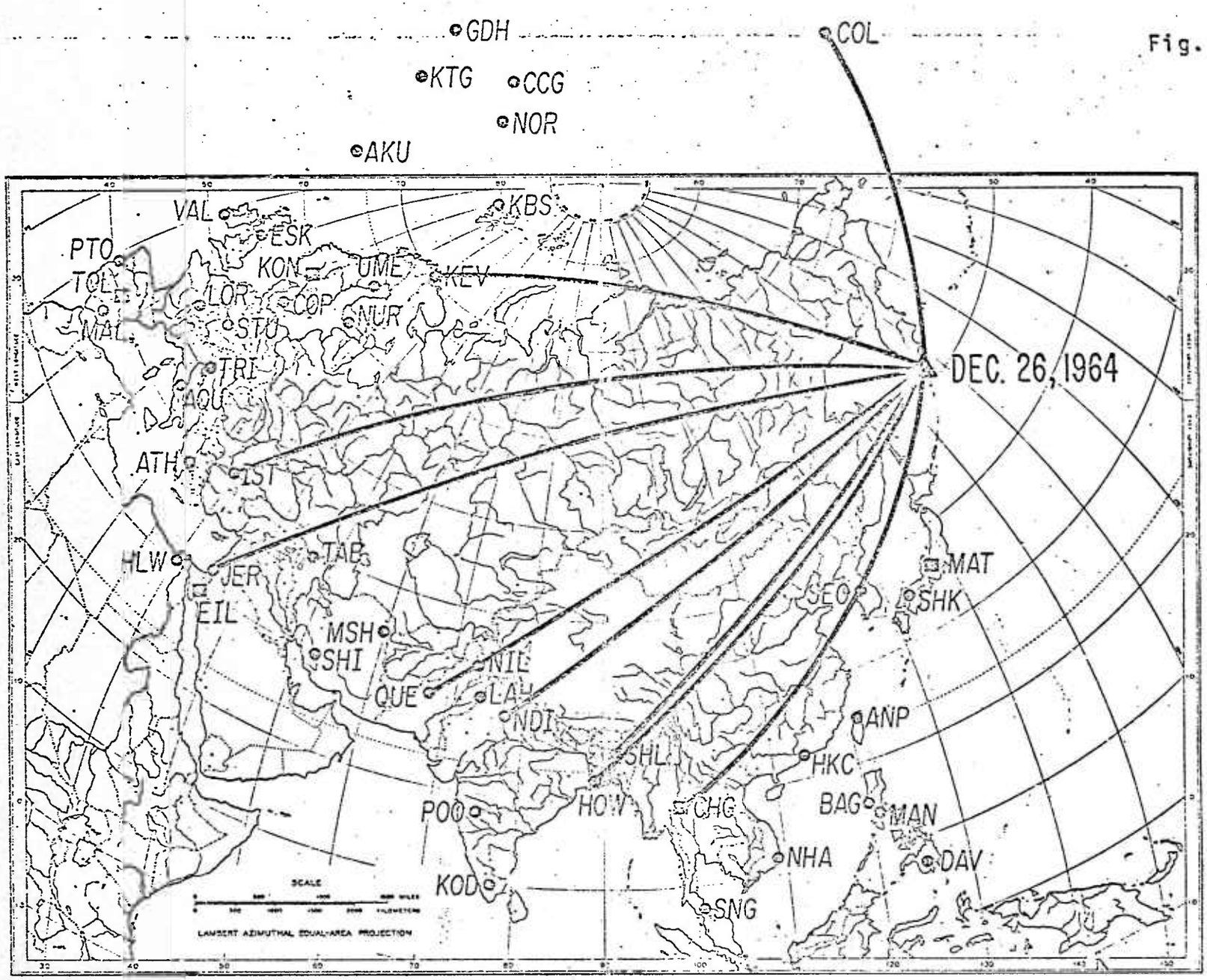

WWSSN STATIONS
HIGH-GAIN, LONG-PERIOD STATIONS

Fig. 11

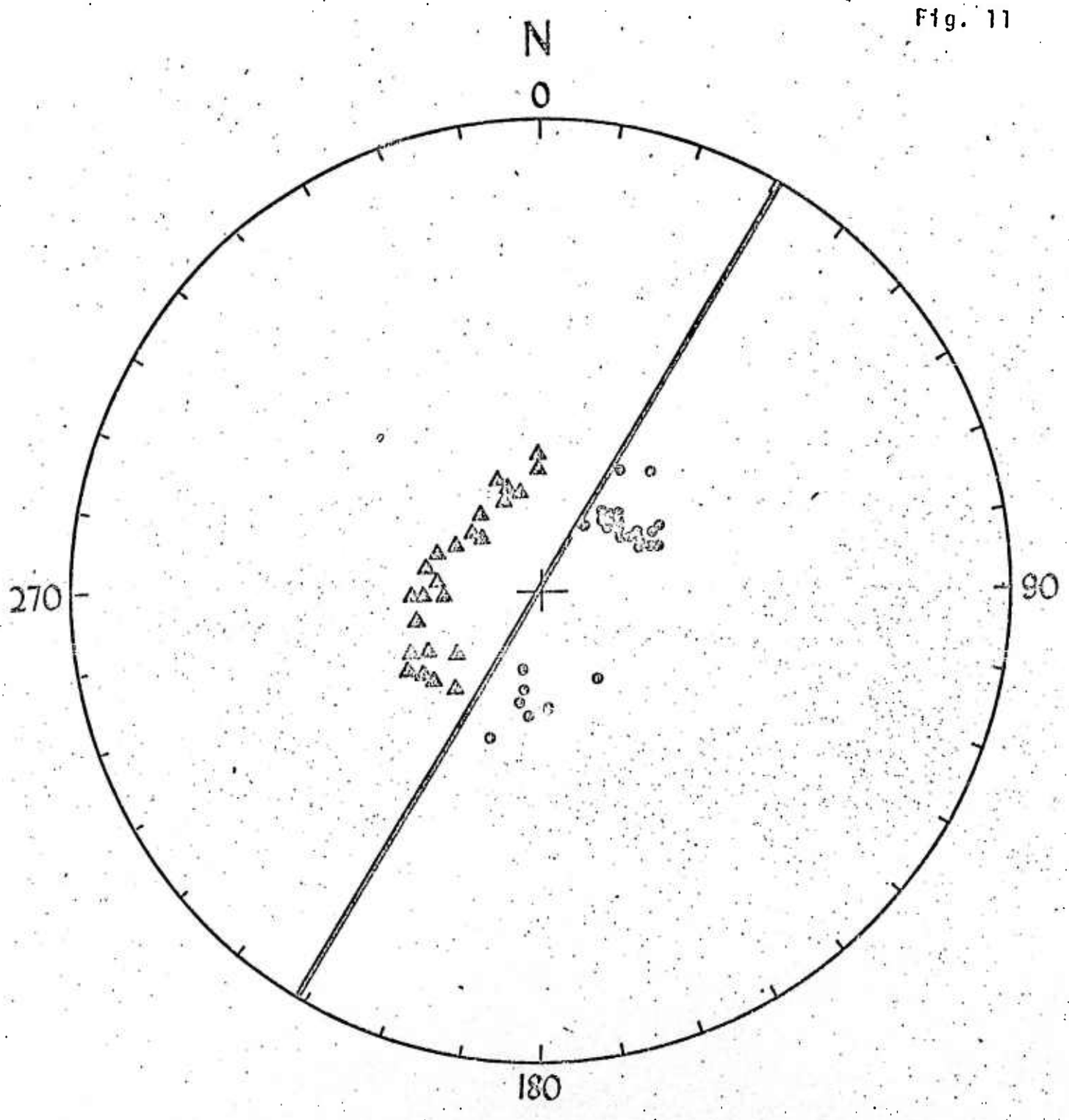

SOURCE DEPTH=136 KM

○ compression

△ dilation

Fig. 12

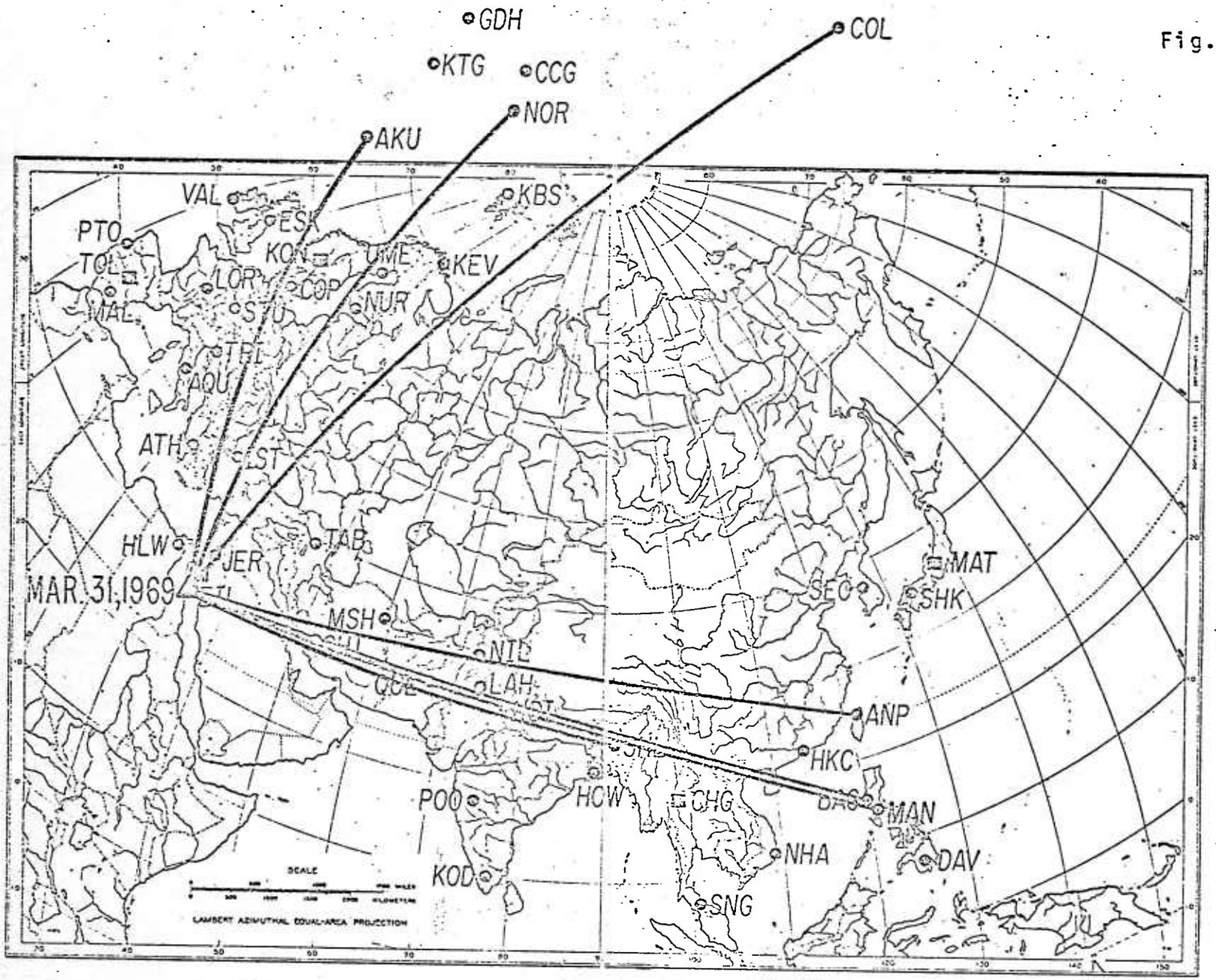

○ WWSSN STATIONS
▣ HIGH-GAIN, LONG-PERIOD STATIONS

Fig. 13

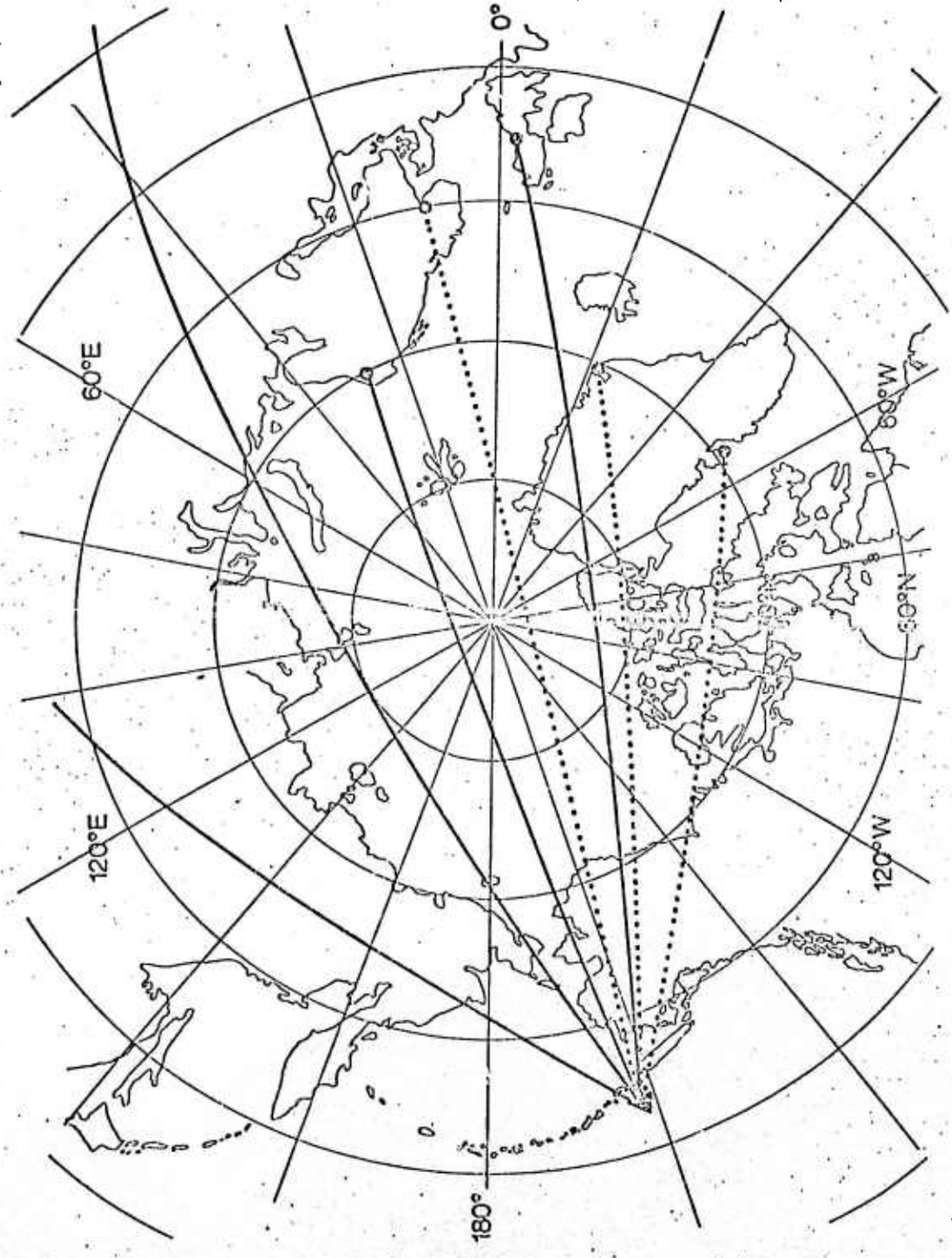

Fig. 14a

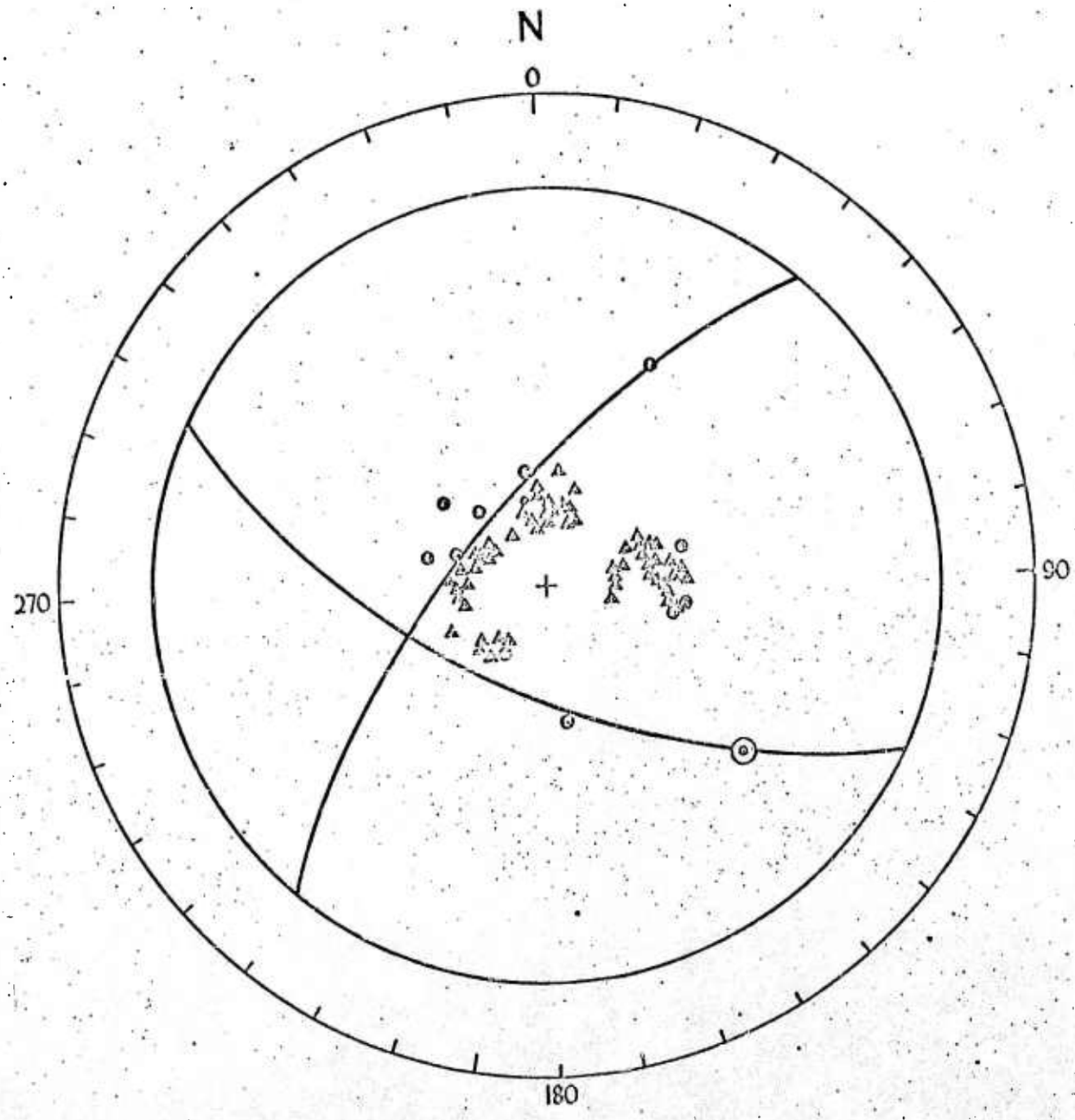

SOURCE DEPTH=33 KM

o · compression

▲ · dilatation

Fig. 14b

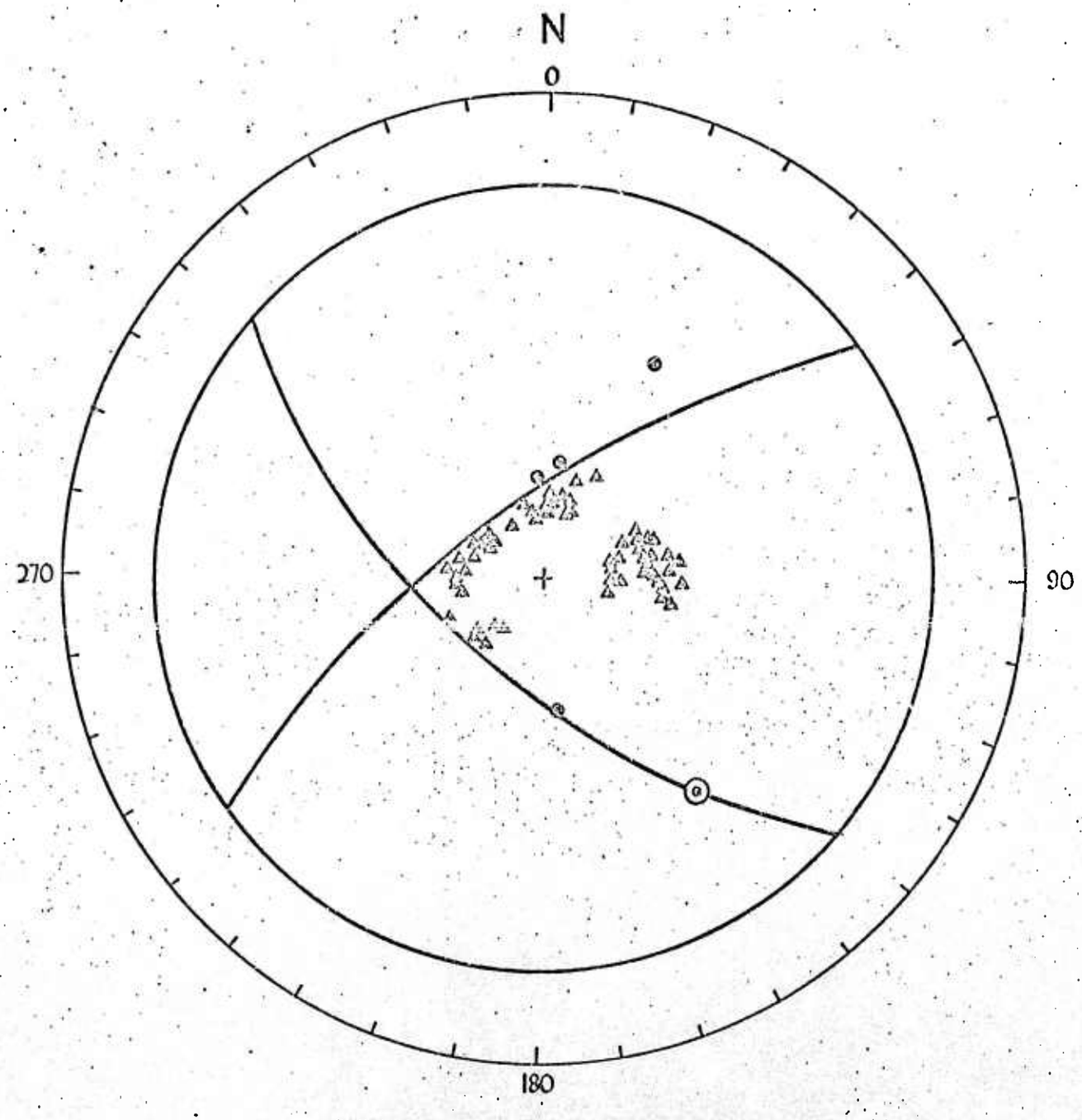

SOURCE DEPTH=33 KM

o compression
Δ dilatation

Fig. 15

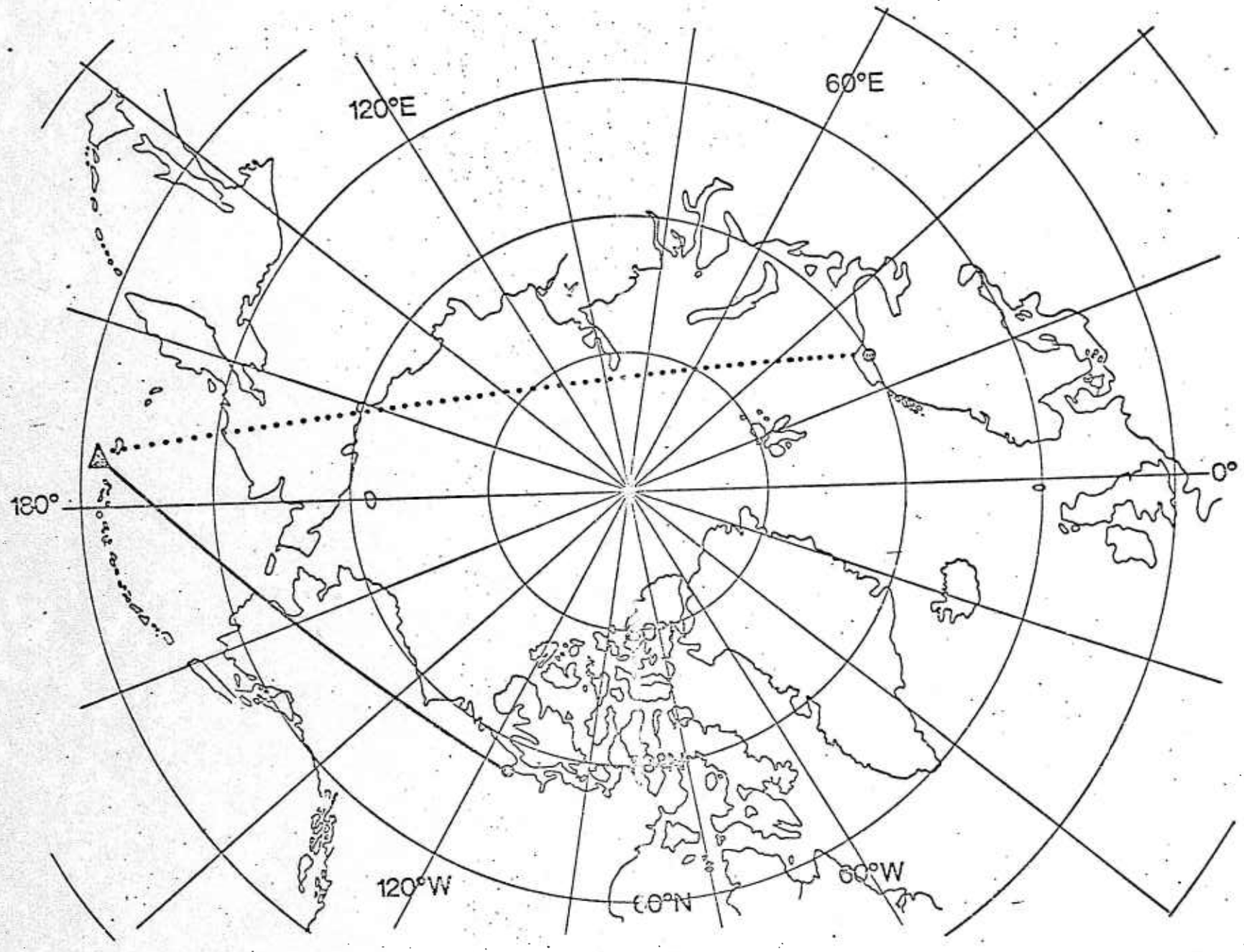

Fig. 16

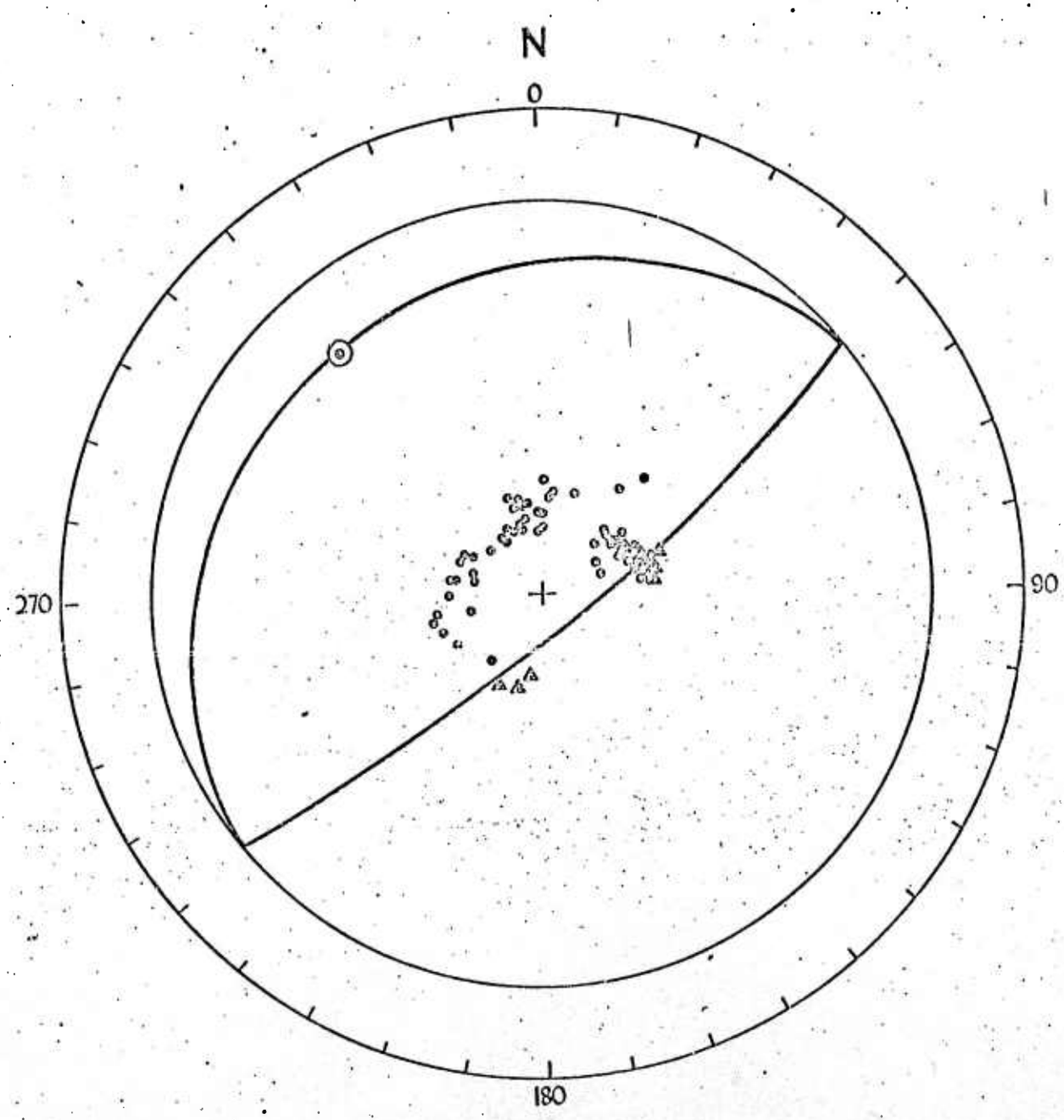

SOURCE DEPTH=41 KM

- compression
- dilatation

Fig. 17

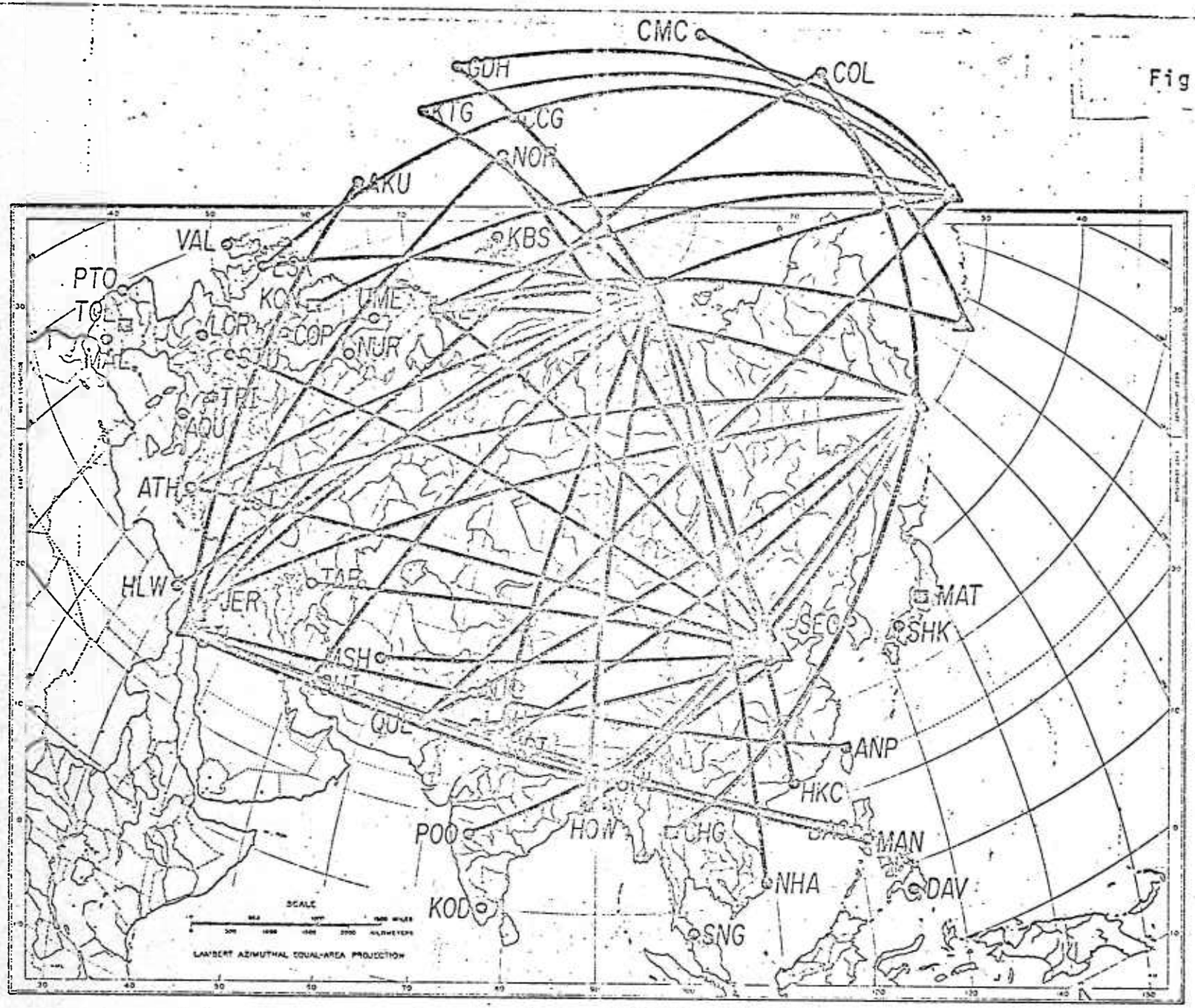

WWSSN STATIONS
HIGH-GAIN, LONG-PERIOD STATIONS

Fig. 18

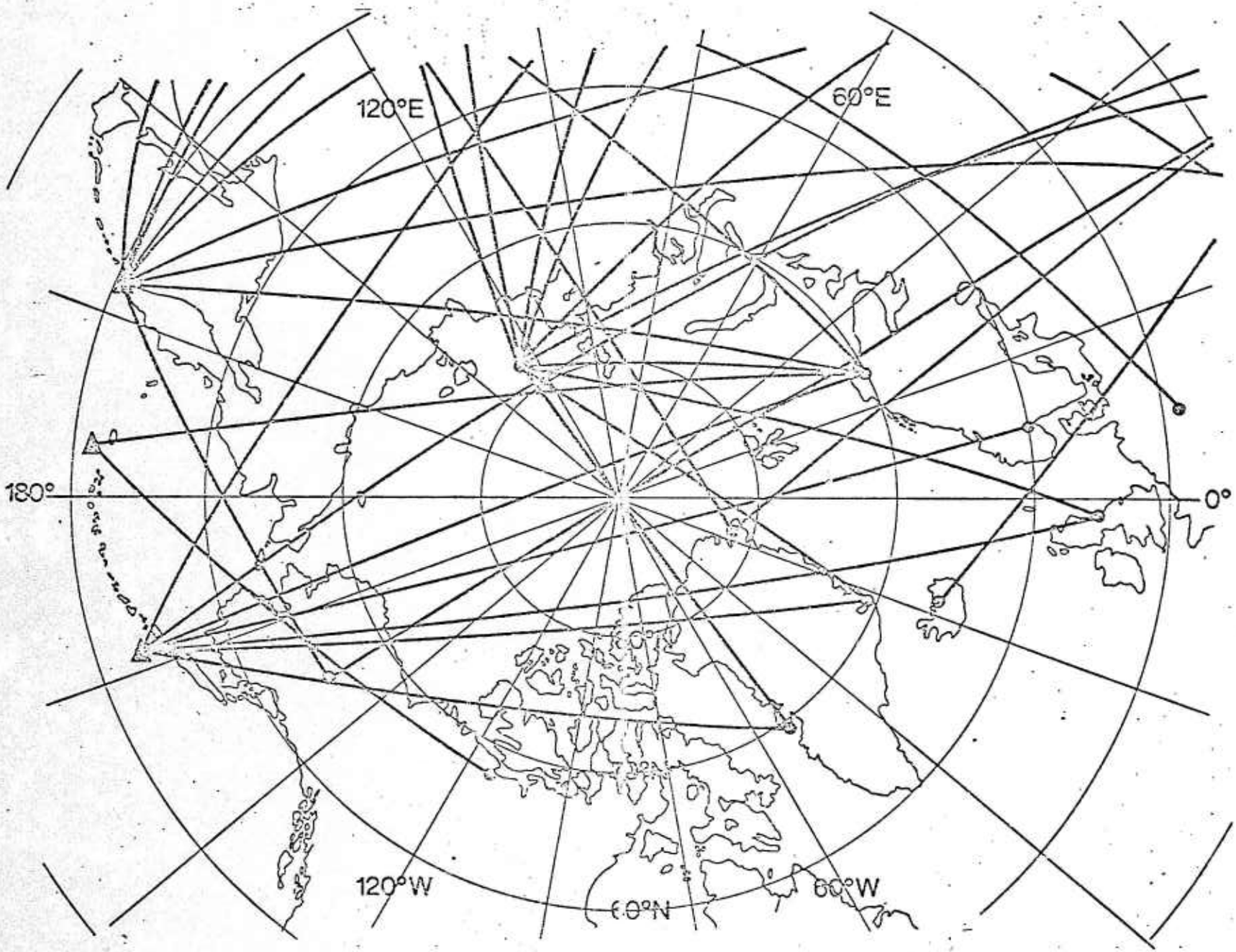

Fig. 19

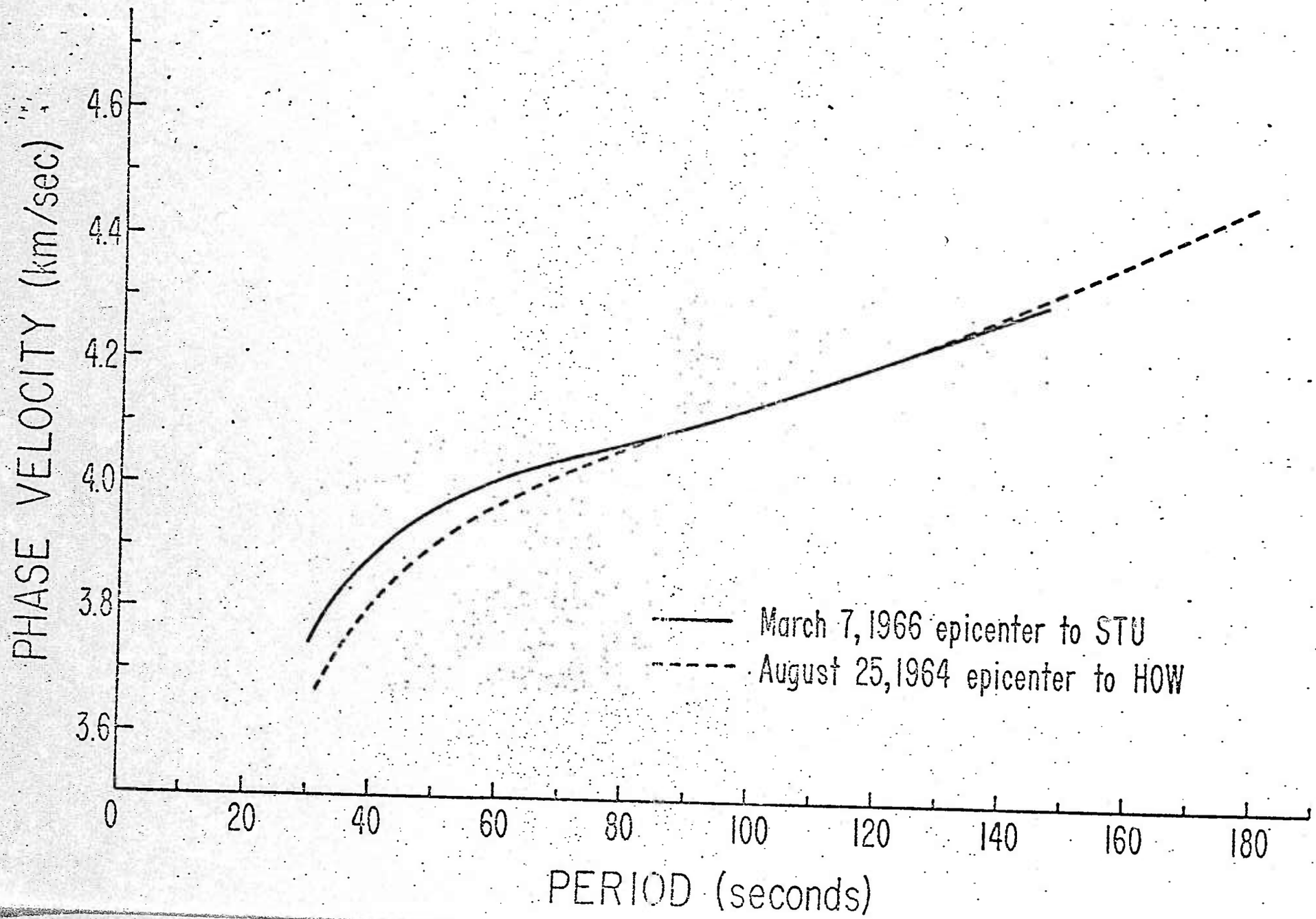
PHASE VELOCITY (km/sec)
4.6
4.4
4.2
4.0
3.8
3.6
0
20
40
60
80
100
120
140
160
180
PERIOD (seconds)
March 7, 1966 epicenter to STU
August 25, 1964 epicenter to HOW

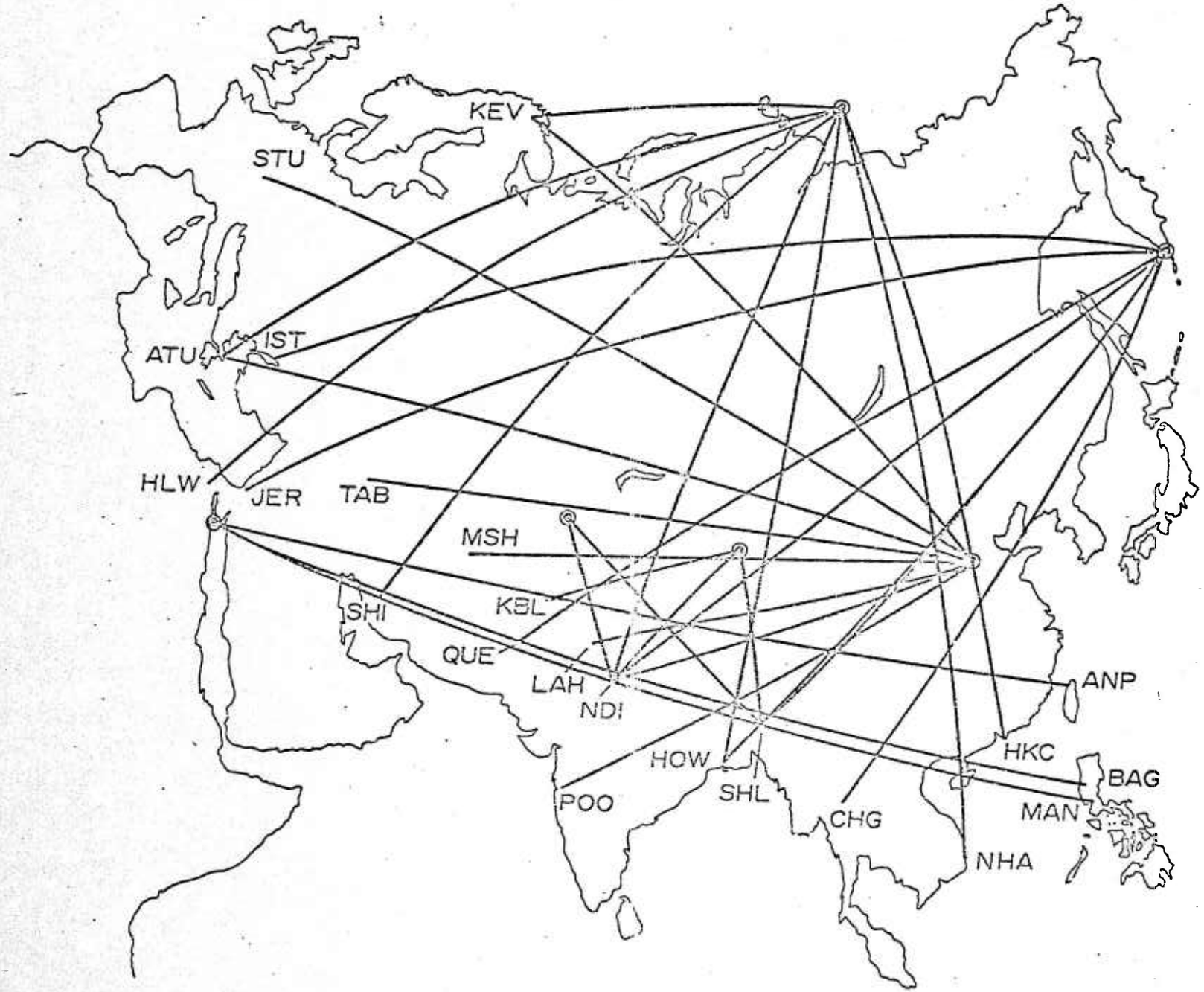
KEV
STU
ATU
IST
HLW
JER
TAB
MSH
SHI
KBL
QUE
LAH
NDI
ANP
HKC
BAG
HOW
SHL
POO
CHG
MAN
NHA

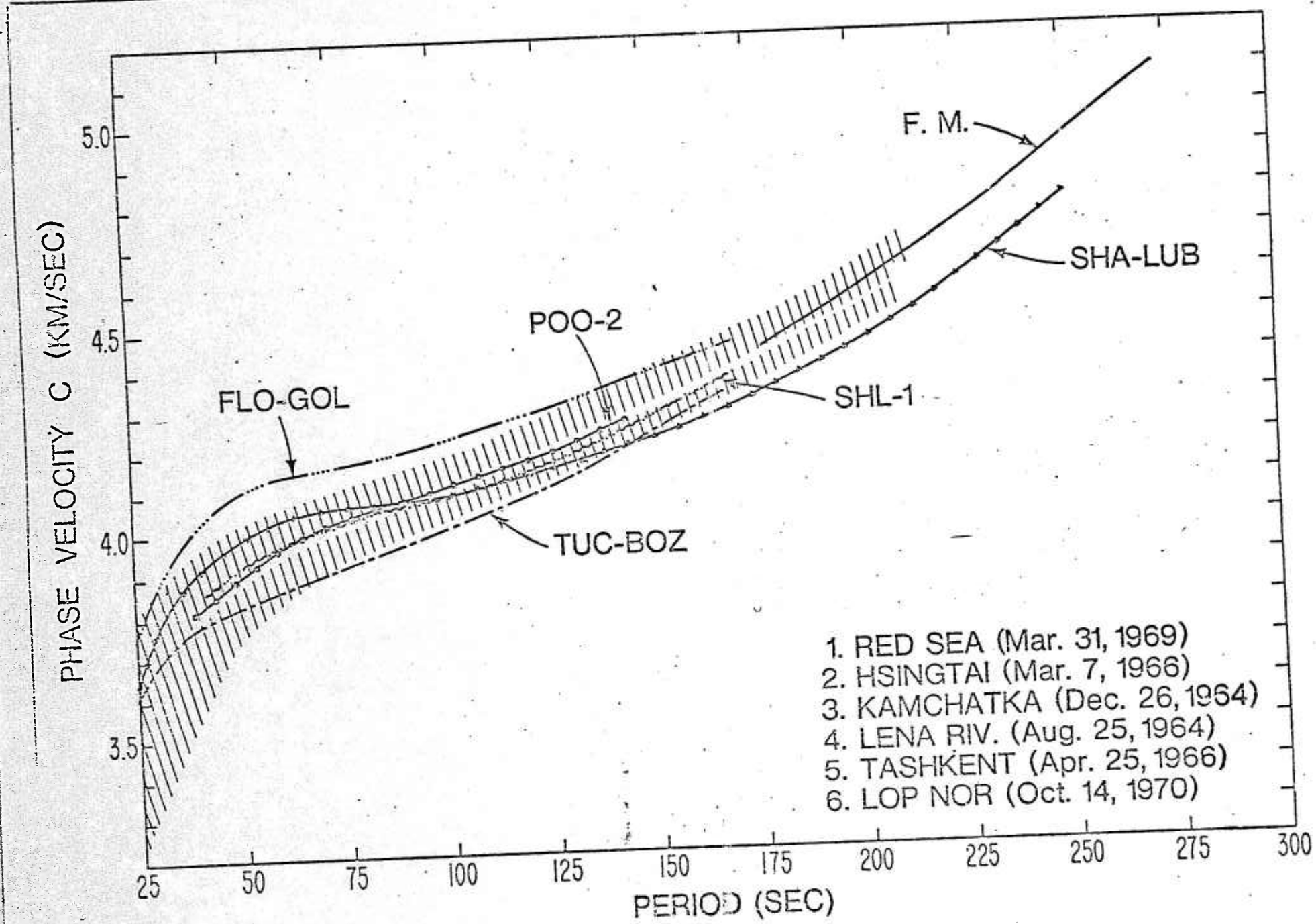
PHASE VELOCITY C (KM/SEC)
5.0
4.5
4.0
3.5
25
50
75
100
125
150
175
200
225
250
275
300
PERIOD (SEC)
F. M.
SHA-LUB
POO-2
SHL-1
FLO-GOL
TUC-BOZ
1. RED SEA (Mar. 31, 1969)
2. HSINGTAI (Mar. 7, 1966)
3. KAMCHATKA (Dec. 26, 1964)
4. LENA RIV. (Aug. 25, 1964)
5. TASHKENT (Apr. 25, 1966)
6. LOP NOR (Oct. 14, 1970)

Fig. 22

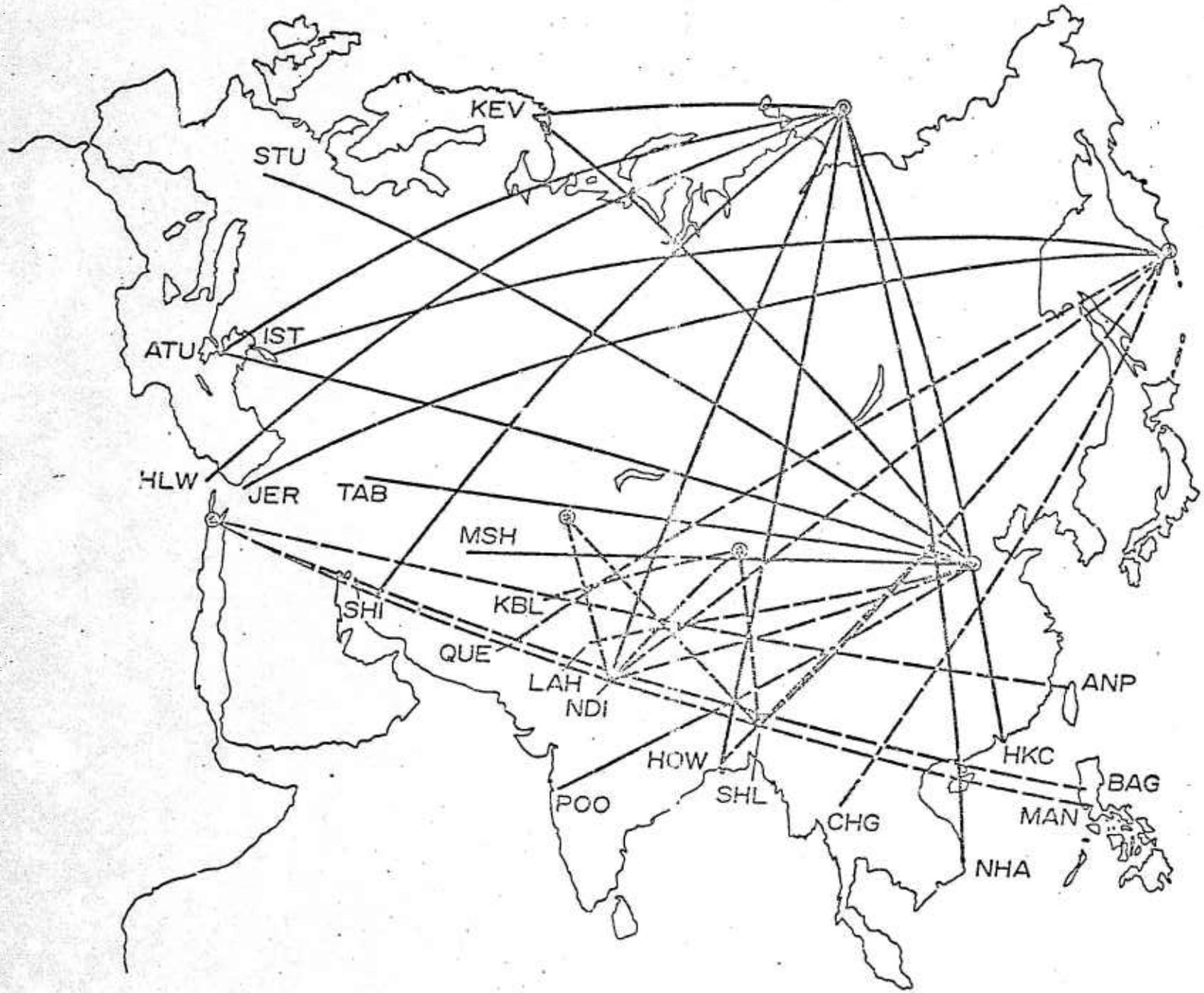
KEV
STU
ATU
IST
HLW
JER
TAB
MSH
SHI
KBL
QUE
LAH
NDI
ANP
HOW
HKC
BAG
POO
SHL
CHG
MAN
NHA

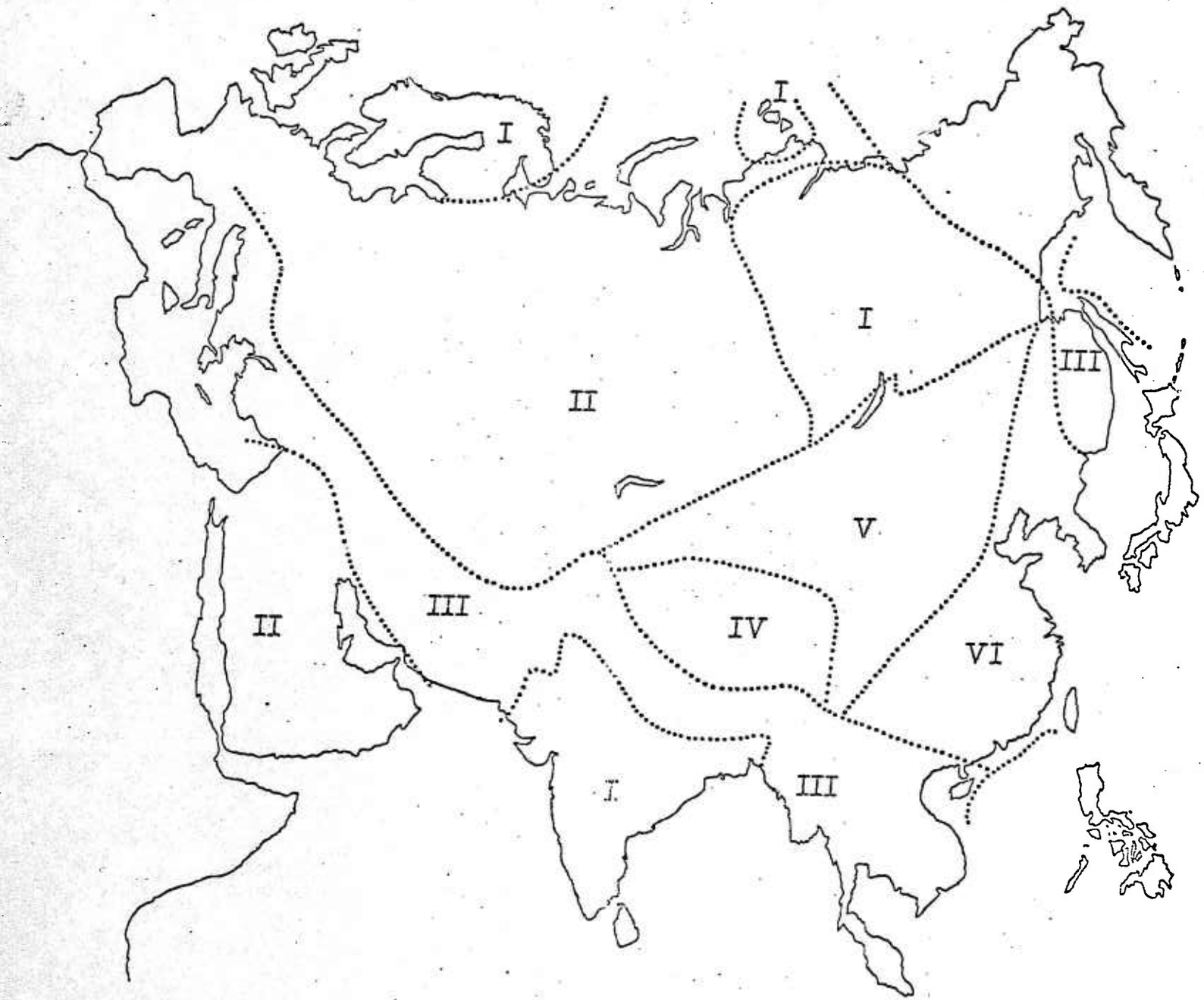
I
I
I
II
III
V
II
III
IV
VI
I
III

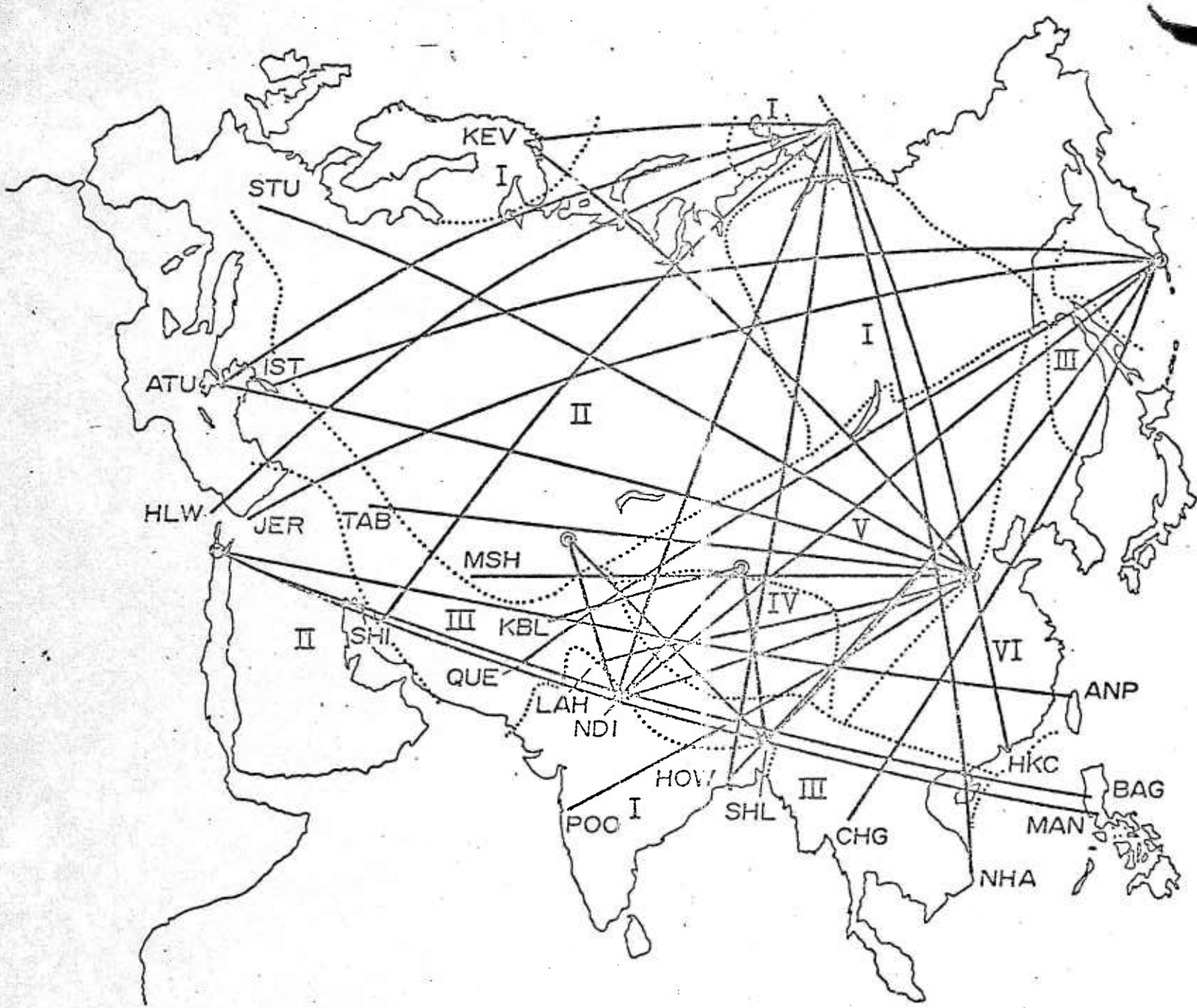
KEV
STU
ATU
IST
HLW
JER
TAB
MSH
SHI
KBL
QUE
LAH
NDI
POO
HOW
SHL
CHG
NHA
HKC
ANP
BAG
MAN
I
II
III
IV
V
VI

UNCLASSIFIED

SECURITY CLASSIFICATION OF THIS PAGE (When Data Entered)

REPORT DOCUMENTATION PAGE	READ INSTRUCTIONS BEFORE COMPLETING FORM
1. REPORT NUMBER AFOSR - TR - 76 - 1027	2. GOVT ACCESSION NO. / 3. RECIPIENT'S CATALOG NUMBER
4. TITLE (and Subtitle) (6) REGIONALIZATION OF THE ARCTIC REGION, SIBERIA AND EURASIAN CONTINENTAL AREA.	5. TYPE OF REPORT & PERIOD COVERED: Scientific Final 6. PERFORMING ORG. REPORT NUMBER
7. AUTHOR(s) (10) Leon Knopoff	8. CONTRACT OR GRANT NUMBER(s) (15) F44620-73-C-0048 // ARPA Order-1827
9. PERFORMING ORGANIZATION NAME AND ADDRESS: University of California, Los Angeles, Institute of Geophysics and Planetary Physics, Los Angeles, California 90024	10. PROGRAM ELEMENT, PROJECT, TASK AREA & WORK UNIT NUMBERS: A.O.1827-33 62701E 6E10
11. CONTROLLING OFFICE NAME AND ADDRESS: ARPA, 1400 Wilson Blvd., Arlington VA 22209	12. REPORT DATE (11) 31 May 1976 13. NUMBER OF PAGES: 79
14. MONITORING AGENCY NAME & ADDRESS (if different from Controlling Office): AFOSR/NP, Bolling AFB Bldg. 410, Wash DC 20332 (9) Final rept. 1 Mar 73 - 31 May 76	15. SECURITY CLASS. (of this report): Unclassified 15a. DECLASSIFICATION/DOWNGRADING SCHEDULE
16. DISTRIBUTION STATEMENT (of this Report) (12) 87 p. (18) AFOSR (19) TR-76-1027	
17. DISTRIBUTION STATEMENT (of the abstract entered in Block 20, if different from Report): Approved for public release; distribution unlimited.	
18. SUPPLEMENTARY NOTES: TECH, OTHER	
19. KEY WORDS (Continue on reverse side if necessary and identify by block number)	

20. ABSTRACT (Continue on reverse side if necessary and identify by block number)

In this investigation, the first purpose was the regionalization of the Arctic region, Siberia and the Eurasian continental area using seismic surface waves. This regionalization determines the structural properties of the upper few hundred kilometers of the earth, and the variation of these properties from one subregion to another in the area under investigation. Once the structural properties in the various regions had been obtained, the second purpose was to apply optimized computer techniques to the computation of accurate theoretical seismograms for any hypothetical type of source located anywhere within this

DD FORM 1 JAN 73 1473 EDITION OF 1 NOV 65 IS OBSOLETE UNCLASSIFIED 181 550 LB

SECURITY CLASSIFICATION OF THIS PAGE (When Data Entered)

continental area. These theoretical seismograms can be applied directly to the discrimination problem by comparing seismograms, computed for both earthquakes and underground explosions with the actual recorded seismogram